Differentiation xxx (xxxx) xxx

Contents lists available at ScienceDirect

Differentiation

journal homepage: www.elsevier.com/locate/diff

Steroidogenic factor 1 (*NR5A1*) induces multiple transcriptional changes during differentiation of human gonadal-like cells

Kirsi Sepponen [a], Karolina Lundin [a], Dawit A. Yohannes [a,b], Sanna Vuoristo [c], Diego Balboa [d,1], Matti Poutanen [e,f], Claes Ohlsson [f], Steinar Hustad [g,h], Ersilia Bifulco [g,i], Pauliina Paloviita [c], Timo Otonkoski [d], Olli Ritvos [j], Kirsi Sainio [k], Juha S. Tapanainen [a,l,*,1], Timo Tuuri [a,1]

[a] Department of Obstetrics and Gynecology, University of Helsinki and Helsinki University Hospital, Helsinki, Finland
[b] Research Programs Unit, Translational Immunology & Department of Medical and Clinical Genetics, University of Helsinki, Helsinki, Finland
[c] Department of Obstetrics and Gynecology, Functional Embryo Genomics Lab, University of Helsinki and Helsinki University Hospital, Helsinki, Finland
[d] Stem Cells and Metabolism Research Program and Children's Hospital, Faculty of Medicine, University of Helsinki, Helsinki, Finland
[e] Research Centre for Integrative Physiology and Pharmacology, Institute of Biomedicine, Faculty of Medicine, University of Turku, Turku, Finland
[f] Centre for Bone and Arthritis Research, Department of Internal Medicine and Clinical Nutrition, Institute of Medicine, Sahlgrenska Academy, University of Gothenburg, Gothenburg, Sweden
[g] Core Facility for Metabolomics, University of Bergen, Bergen, Norway
[h] Department of Clinical Science, University of Bergen, Bergen, Norway
[i] Department of Biological Sciences, University of Bergen, Bergen, Norway
[j] Department of Physiology, Faculty of Medicine, University of Helsinki, Helsinki, Finland
[k] Department of Biochemistry and Developmental Biology, Faculty of Medicine, University of Helsinki, Helsinki, Finland
[l] Department of Obstetrics and Gynecology, University Hospital of Oulu, University of Oulu, Medical Research Center Oulu and PEDEGO Research Unit, Oulu, Finland

ARTICLE INFO

Keywords:
CRISPR
Gonadal development
Infertility
Sertoli cell
SF1
Testis

ABSTRACT

Nuclear receptor subfamily 5 group A member 1 (*NR5A1*) encodes steroidogenic factor 1 (SF1), a key regulatory factor that determines gonadal development and coordinates endocrine functions. Here, we have established a stem cell-based model of human gonadal development and applied it to evaluate the effects of *NR5A1* during the transition from bipotential gonad to testicular cells. We combined directed differentiation of human induced pluripotent stem cells (46,XY) with activation of endogenous *NR5A1* expression by conditionally-inducible CRISPR activation. The resulting male gonadal-like cells expressed several Sertoli cell transcripts, secreted anti-Müllerian hormone and responded to follicle-stimulating hormone by producing sex steroid intermediates. These characteristics were not induced without *NR5A1* activation. A total of 2691 differentially expressed genetic elements, including both coding and non-coding RNAs, were detected immediately following activation of *NR5A1* expression. Of those, we identified novel gonad-related putative *NR5A1* targets, such as SCARA5, which we validated also by immunocytochemistry. In addition, *NR5A1* activation was associated with dynamic expression of multiple gonad- and infertility-related differentially expressed genes. In conclusion, by combining targeted differentiation and endogenous activation of *NR5A1* we have for the first time, been able to examine in detail the effects of *NR5A1* in early human gonadal cells. The model and results obtained provide a useful resource for future investigations exploring the causative reasons for gonadal dysgenesis and infertility in humans.

* Corresponding author. Department of Obstetrics and Gynecology, Helsinki University Hospital and Helsinki University, P.O. Box 140, 00029 HUS, Finland.
E-mail address: juha.tapanainen@helsinki.fi (J.S. Tapanainen).
[1] Current affiliation: Bioinformatics and Genomics Program, Centre for Genomic Regulation, The Barcelona Institute of Science and Technology, Barcelona, Spain.
[2] These authors have contributed equally to this work and share last authorship.

https://doi.org/10.1016/j.diff.2022.08.001
Received 19 April 2022; Received in revised form 14 August 2022; Accepted 14 August 2022
Available online 30 August 2022

Abbreviations

AMH	anti-Müllerian hormone
BMP	bone morphogenetic protein
cAMP	3′,5′-cyclic adenosine monophosphate
CTD	Comparative Toxicogenomics Database
DAPI	4′,6-diamidino-2-phenylindole
DE	differential expression (of gene/feature)
DOX	doxycycline hyclate
FBS	fetal bovine serum
FC	fold change
FSH	follicle-stimulating hormone
FSHR	follicle-stimulating hormone receptor
GC	granulosa cell
hiPSC	human induced pluripotent stem cell
INHA	inhibin subunit alpha
IPA	Ingenuity Pathway Analysis Knowledge Base
LC	Leydig cell
LH	luteinizing hormone
LHCGR	luteinizing hormone/choriogonadotropin receptor
LLOQ	lower limit of quantification
NR5A1	nuclear receptor subfamily 5 group A member 1
SC	Sertoli cell
SCARA5	scavenger receptor class A member 5
SF1	steroidogenic factor 1
SOX9	SRY-box transcription factor 9
PBS	phosphate-buffered saline solution
qRT-PCR	quantitative reverse transcription PCR
TMP	trimethoprim

1. Introduction

Gonads arise as a pair of thickenings of the coelomic epithelium on the ventromedial surface of the mesonephros between the fifth and the sixth week of development in humans (Satoh, 1991). Gonads are initially bipotential, *i.e.* capable of developing into testes or ovaries (DeFalco and Capel, 2009). The anatomical sex of the gonads is determined by the presence or absence of a sex-determining gene SRY. In males, SRY initiates testicular development by activating SRY-box transcription factor 9 (SOX9, Chaboissier et al., 2004). In females, absence of SRY leads to maintenance of WNT4 expression, thus facilitating ovarian differentiation (Vainio et al., 1999; Tang et al., 2020).

The bipotential gonads and the different gonadal cell lineages that arise from them are characterized by expression of multiple transcription factors (Rotgers et al., 2018; Sasaki et al., 2021) including steroidogenic factor 1 (SF1, also known as AD4BP and FTZF1), which is crucial for early gonadal development (Luo et al., 1994; Sadovsky et al., 1995). SF1 is encoded by nuclear receptor subfamily 5 group A member 1 (*NR5A1*), a member of the nuclear receptor superfamily (Mullican et al., 2013). In mice, NR5A1 expression can first be detected in bipotential gonads at 9.5–10.2 days post coitum (Ikeda et al., 1994, 2001; Hu et al., 2013) and in humans in a pool of cells underlying the genital ridge between the fourth and the fifth week of development (Hanley et al., 1999). In males, NR5A1 continues to be expressed in the progenitors of steroidogenic Leydig cells (LCs), interstitial cells, and germ-cell supporting Sertoli cells (SCs, Schmahl et al., 2000; Stévant et al., 2018). NR5A1 upregulates SOX9, a marker of early SCs, together with SRY and thereby augments gonadal masculinization and SC differentiation (Sekido and Lovell-Badge, 2008; She and Yang, 2017). NR5A1 is also required for SC survival post sex determination (Anamthathmakula et al., 2019). Recently, a conditional deletion of *Nr5a1* in rodents has been reported to impair testicular development and instead, induce ovarian identity (Ikeda et al., 2021). The role of NR5A1 in fetal ovaries is not clear, but NR5A1-positive progenitor cells give rise to pre-granulosa and granulosa cells (GCs) in mice (Stévant et al., 2019). NR5A1 also triggers the expression of steroidogenic enzymes in both male and female gonads (Givens et al., 1994; Michael et al., 1995; Zhang and Mellon, 1996; Hu et al., 2001). Although NR5A1 regulates several factors associated with steroidogenesis and gonad development, targets of this key master regulator at different stages of fetal gonad development and function remain to be identified.

In mice, *Nr5a1* knockout leads to degeneration of gonads and adrenal glands, XY sex reversal with persistent Müllerian structures, and postnatal lethality due to adrenal insufficiency (Luo et al., 1994; Sadovsky et al., 1995; Morohashi and Omura, 1996). *Nr5a1* overexpression drives formation of ectopic adrenal tissue and adrenal tumorigenesis (Doghman et al., 2007; Zubair et al., 2009; Almeida et al., 2010). In contrast, a heterozygous deletion of *Nr5a1* in mice affects adrenal development but gonadal development remains undisrupted (Bland et al., 2000, 2004). In humans, even mild disruptions in *NR5A1* integrity may have a pronounced impact as already a single heterozygous mutation in *NR5A1* may lead to gonadal dysgenesis or 46,XY sex reversal (Achermann et al., 1999; Mallet et al., 2004). In males the mutation phenotype typically involves atypical genitalia, partial or complete sex reversal or infertility (Bashamboo et al., 2010; Domenice et al., 2016; Fabbri-Scallet et al., 2020). In females, the phenotype may range from atypical genitalia to primary ovarian failure (Lourenço et al., 2009; Camats et al., 2012; Domenice et al., 2016).

We previously published a protocol describing differentiation of human embryonic stem cells into bipotential gonadal cells, characterized by timely expression of *GATA4*, *WT1*, *EMX2*, and *LHX9* (Sepponen et al., 2017). However, *NR5A1* was not expressed in these cells. Here we demonstrate how induction of *NR5A1* promotes differentiation into more mature gonadal-like cells with steroidogenic capacity and capability to respond to hormonal stimulation. Additionally, we identified various *NR5A1* target candidates possibly regulating human gonadal development.

2. Results

2.1. NR5A1 induces expression of somatic gonadal markers

To examine the role of *NR5A1* during embryonic gonadal development, CRISPR-Cas9 gene activation technology was employed to induce endogenous *NR5A1* expression in human induced pluripotent stem cells (hiPSCs) during directed gonadal differentiation. In this context, a catalytically inactive form of Cas9 (dCas9) fused with a transactivator domain binds to the target gene promoter to induce target gene transcription. dCas9 expression is controlled with doxycycline (DOX). An additional destabilization domain attached to dCas9 leads, without stabilizing trimethoprim (TMP) administration, degradation of the dCas9 protein preventing unwanted target gene activation due to leakiness of the DOX-controlled dCas9 promoter (Balboa et al., 2015). Experiments were performed with the HEL46.11-DDdCas9Vp192-NR5A1 clone 14 sub-line according to an extended version (Fig. 1A) of the protocol published earlier (Sepponen et al., 2017). Briefly, hiPSCs expressing pluripotency marker *OCT4* (Supplementary Fig. S1) were differentiated with Activin A, Wnt-agonist CHIR99021 and sequential activation and inhibition of bone morphogenetic protein (BMP) signaling in a monolayer culture. Within 24 h, expression of the pluripotency marker *OCT4* was decreased and primitive streak-like stage was induced, followed by upregulation of intermediate mesoderm markers by day 4 (Supplementary Fig. S1). At this point, the 6-day activation of *NR5A1* with DOX and TMP (+DOX+TMP) was initiated

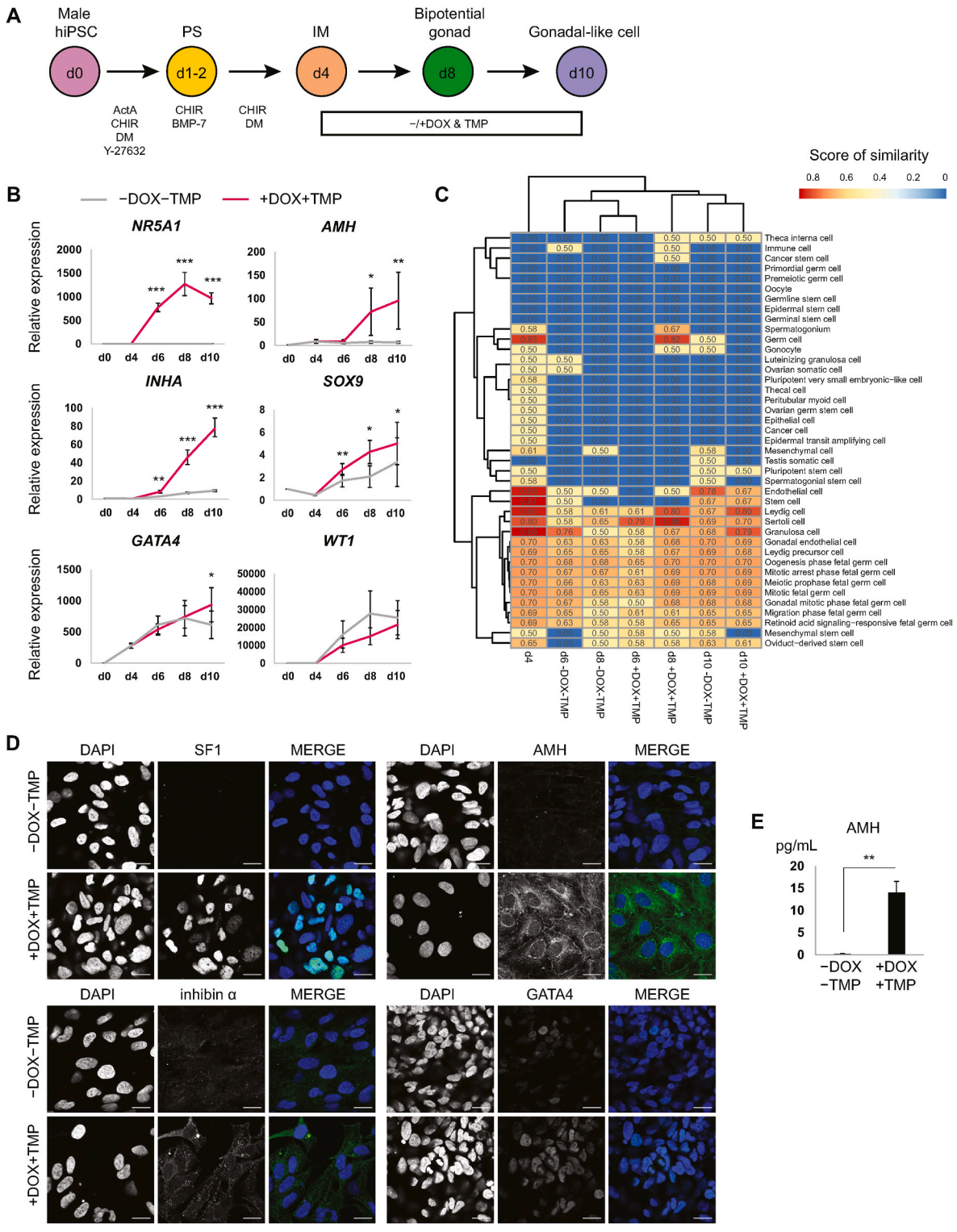

Fig. 1. NR5A1 promotes differentiation of male hiPSCs into gonadal-like cells. **(A)** A schematic illustration of hiPSC differentiation to gonadal-like cells with applied molecular compounds and related developmental stages. **(B)** mRNA levels analyzed by quantitative reverse transcription polymerase chain reaction revealed the relative expression of markers associated with early testis (*NR5A1*, *AMH*, *INHA*, *SOX9*) and bipotential gonad (*NR5A1*, *GATA4*, *WT1*) at the indicated days of differentiation. Each sample represents mean ± SEM (n=6). Gene-expression levels are quantified relative to undifferentiated hiPSCs (*$P<0.05$, **$P<0.01$, ***$P<0.001$, Mann Whitney *U* test with mean ranks). **(C)** Whole transcriptome sequencing of NR5A1-induced and non-induced differentiated cells at indicated days followed by annotation of cell types in each sample cluster by using a cluster-based automatic cell annotation tool (scCATCH). Values indicate scores of similarity. **(D)** Confocal microscopy of immunolabeled non-induced (-DOX-TMP) and induced (+DOX+TMP) cells demonstrating expression of SF1, AMH, inhibin subunit α, and GATA4 at day 10 of differentiation. 4′,6-diamidino-2-phenylindole (DAPI) was used to stain cell nuclei. Individual channels were combined in merge with DAPI (blue) and SF1, AMH, inhibin subunit α, or GATA4 (green). Images were taken from representative areas. Scale bars 20 μm. **(E)** Human AMH secretion at day 10 of differentiation in the absence (-DOX-TMP) or presence (+DOX+TMP) of *NR5A1* activation. Each bar value represents mean ± SEM (n=3, **$P<0.01$, independent samples *t*-test). ActA, Activin A; BMP, Bone morphogenetic protein; CHIR, CHIR-99021; d, day of differentiation; DM, dorsomorphin; DOX, doxycycline hyclate; hiPSC, human induced pluripotent stem cell; IM, intermediate mesoderm; PS, primitive streak; TMP, trimethoprim.

and a significant increase in *NR5A1* mRNA expression was detected on day 6 (Mann Whitney *U* test, *P*=5.128E-6), day 8 (*P*=3.333E-6), and day 10 (*P*=5.128E-6) of differentiation as analyzed by quantitative reverse transcription PCR (qRT-PCR, n=6, Fig. 1B). Moreover, expression of anti-Müllerian hormone (*AMH*), a fetal SC marker (Tran et al., 1977; Rajpert-De Meyts et al., 1999), increased on days 8 and 10 [Mann Whitney *U* test, *P* (day 6)=0.533, *P* (day 8)=0.038, *P* (day 10)=0.002, n=6, Fig. 1B]. Likewise, the expression of early SC markers inhibin subunit alpha (*INHA*) and *SOX9* at days 6–10 increased in induced cells, whereas in the non-induced cells the expression levels of these gonadal genes remained low (Fig. 1B).

To more specifically analyze the effects of NR5A1 expression during differentiation at the transcriptional level, we performed RNA sequencing analyses of NR5A1-induced and non-induced cells on days 4, 6, 8, and 10 of differentiation. Based on an annotation analysis conducted using single-cell Cluster-based Automatic Annotation Toolkit for Cellular Heterogeneity (scCATCH, Shao et al., 2020), the cells at day 4 of differentiation were predicted to be fairly heterogeneous, representing a mixture of genital ridge-type cells while the most likely cell types present in the NR5A1-induced samples at days 6, 8 and 10 were SCs, LCs, or GCs (Fig. 1C, Supplementary Table 1). Without NR5A1 induction the gonadal development was evident but not as targeted as with the induction, as measured by the studied markers. Thus, activation of *NR5A1* expression in bipotential gonadal-like cells seems to promote differentiation of somatic cell types of gonads.

The staining intensities of SF1, AMH, and inhibin subunit α increased after induction, as observed by immunocytochemistry at day 10 of differentiation (Fig. 1D). Without *NR5A1* activation, SF1-positive cells were not detected, and only faint signals were observed for AMH and inhibin subunit α. Furthermore, at day 10 of differentiation NR5A1-induced cells secreted AMH at significantly higher concentrations than non-induced cells, in which AMH secretion was almost undetectable (Fig. 1E, independent *t*-test, 2-tailed, *P*=0.003, n=3).

Of known crucial transcription factors regulating gonadal development, *WT1* (Kreidberg et al., 1993; Chen et al., 2017) was not affected by *NR5A1* activation and was expressed at similar levels in both groups during the differentiation (Fig. 1B). On the other hand, GATA4 exhibited slightly higher expression levels in NR5A1-induced cells both at mRNA and protein levels at day 10 of differentiation (Fig. 1B and D, Supplementary Data 1). These results demonstrated that activation of *NR5A1* induced the expression of somatic gonadal markers and promoted differentiation into somatic gonadal-like cells.

2.2. *NR5A1* induces steroidogenesis in hiPSC-derived male gonadal-like cells

NR5A1 activation induced mRNA expression of several key genes encoding steroidogenic enzymes (Miller and Auchus, 2011). The expression of *CYP11A1* and *HSD3B2* on days 6–10 increased dramatically in response to NR5A1 (Fig. 2A). In addition, *CYP17A1* was upregulated on days 8 and 10 in the induced cells. Instead, *NR5A1* activation did not strongly affect *CYP19A1*, although its expression was higher on days 6–10 when compared with non-induced cells (Fig. 2A). *HSD17B3* encodes 17β-hydroxysteroid dehydrogenase 3, an enzyme found in fetal and newborn SCs and adult LCs, but not expressed in early fetal LCs in humans or in fetal LCs in mice (Guo et al., 2021; O'Shaughnessy et al., 2000; Shima et al., 2013). *HSD17B3* was significantly upregulated in induced cells when compared with non-induced cells on days 8 and 10, as demonstrated by qRT-PCR [Mann Whitney *U* test, *P* (day 6)=0.065, *P* (day 8)=0.0098, *P* (day 10)=6.958E-5, n=6]. Furthermore, the expression of steroidogenesis-related *STAR* was upregulated by *NR5A1* activation, but remained at basal level in the non-induced cells on days 6–10 (Fig. 2A). Immunocytochemical staining of the differentiated cells on day 10 revealed increased expression of SF1, StAR, P450SCC, and HSD3B2 in the induced cells, which contrasts with low or missing protein expression in the non-induced cells (Fig. 2B). StAR and P450SCC localized to the cytoplasm of cells expressing SF1 at varying intensities. The percentage of SF1, P450SCC and/or SOX9 positive cells estimated by co-immunolabeling of the differentiated NR5A1-induced cells was: 30.4% (mean±SD 15.7) SF1+ cells, 13% (mean±SD 8.16) SOX9+ cells, 8.7% (mean±SD 1.02) P450SCC+ cells, and 3.1% (mean±SD 3.01) SOX9+P450SCC+ cells (Supplementary Fig. S2A). The non-induced cells expressed SOX9 at levels similar to the NR5A1-induced cells. Thus, based on co-immunolabeling *NR5A1* activation induced steroidogenesis in about 3% of the early male gonadal-like cells expressing SC marker SOX9, and in about 5.6% of gonadal-like cells negative for SOX9. Although variations in SF1 expression levels might induce differences in gonadal marker expression and in the differentiation outcome, these were not studied in detail.

As the gonads and the adrenal glands are derivatives of partially shared regions of intermediate mesoderm (Ikeda et al., 1994; Hatano et al., 1996; Sasaki et al., 2021) and NR5A1 is essential also for adrenal development (Luo et al., 1994; Sadovsky et al., 1995), we assessed the presence of adrenal gland-specific markers. *CYP21A2* and the enzyme it encodes, which is involved in aldosterone and cortisol biosynthesis, are expressed in fetal human adrenal glands but not in the gonads (Voutilainen and Miller, 1986; Turcu and Auchus, 2015; del Valle et al., 2017; Melau et al., 2019). Only moderate upregulation of *CYP21A2* was detected on days 6, 8, and 10 in the induced (+DOX+TMP) cells by qRT-PCR (Fig. 2A). Expression of CYP11B2, a gene encoding aldosterone synthase (Ogishima et al., 1989; Curnow et al., 1991) was negligible and expression levels in fact decreased at all measured time points following *NR5A1* activation (Fig. 2A).

As gonadotropins and their receptors are crucial for testicular development and function and NR5A1 promotes transcription of rat follicle stimulating hormone receptor (*Fshr*) *in vitro* and regulates transcription of luteinizing hormone/choriogonadotropin receptor (*Lhcgr*) in rat GCs (Chen et al., 1999; Heckert, 2001; O'Shaughnessy and Fowler, 2011), changes in the expression levels of *FSHR* and *LHCGR* in the differentiating cells were evaluated in the presence and absence of *NR5A1* activation. Within testes, FSHR can be found in Sertoli cells, while LHCGR is expressed in Leydig cells. However, information about dispersion of these receptors in the very early human testes is scarce. In this study, upregulation of *LHCGR* in NR5A1-induced cells was evident during all time points; indeed, without induction its expression was minimal (Supplementary Fig. S2B). In contrast, *FSHR* was expressed in both NR5A1-induced and non-induced cells. Surprisingly, NR5A1 was found to suppress *FSHR* expression levels (Supplementary Fig. S2B).

We also tested the functionality of FSHR and LHCGR by stimulating the cells with follicle stimulating hormone (FSH) and luteinizing hormone (LH) and measuring the accumulation of 3′,5′-cyclic adenosine monophosphate (cAMP). Both NR5A1-induced and non-induced differentiated cells responded to FSH and forskolin stimulations by producing cAMP (Supplementary Fig. S2C), demonstrating that FSHR was active in the differentiated cells regardless of *NR5A1* induction. In contrast, cells in neither condition responded to stimulation with luteinizing hormone (LH) by producing cAMP (Supplementary Fig. S2C). FSH decreased the level of *FSHR* mRNA transcripts both in the induced and non-induced cells after an 8-h stimulation (Supplementary Fig. S2D). In addition, FSH induced *STAR* expression in non-induced cells but not significantly in the induced cells [ANOVA, Dunnett *t*-test, 2-sided, *P* ($FSH_{-DOX-TMP}$)=0.005, *P* ($FSH_{+DOX+TMP}$)=0.202, n=3]. Forskolin induced *STAR* expression in both conditions. Furthermore, no substantial upregulation of the testicular marker *INHA* was detected following gonadotropin stimulation in either condition.

As expression of steroidogenic enzymes and receptors mediating steroidogenesis were detected in the differentiating cells, we assayed the levels of steroid hormones from conditioned cell culture media on day 8 of differentiation following a 24-h stimulation with FSH, LH, or forskolin directly activating cAMP production. NR5A1-induced cells produced progesterone, 17-hydroxy (OH) progesterone, androstenedione, estradiol, and estrone (Fig. 2C). FSH stimulation further increased their levels

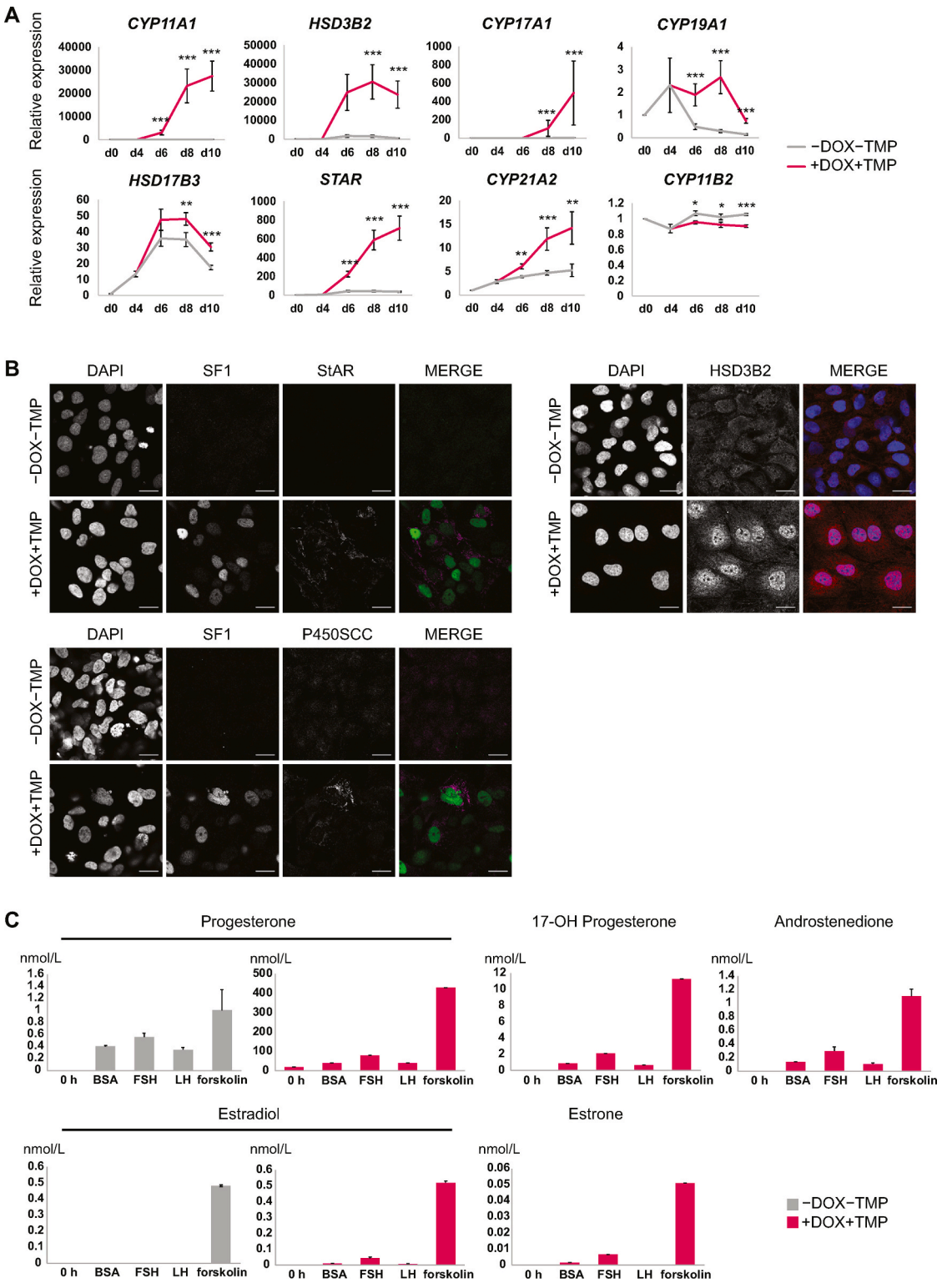

Fig. 2. Steroidogenesis is induced in male gonadal-like cells following *NR5A1* activation. **(A)** Relative mRNA expression of several steroidogenic/steroidogenesis-associated genes of gonads and/or adrenal glands in non-induced (-DOX-TMP) and induced (+DOX+TMP) cells at indicated days. Each sample represents mean ± SEM (n=4–6). Gene-expression levels are quantified relative to undifferentiated hiPSCs (*P<0.05, **P<0.01, ***P<0.001, Mann Whitney U test with mean ranks). **(B)** Confocal microscopy of non-induced (-DOX-TMP) and induced (+DOX+TMP) cells at day 10 of differentiation immunolabeled with antibodies directed against SF1 and StAR (costaining), SF1 and P450SCC, (costaining) or HSD3B2. Individual channels were combined in merge with DAPI (blue) staining cell nuclei and HSD3B2 (red) or with SF1 (green) and StAR/P450SCC (magenta). Images were taken from representative areas. Scale bars 20 μm. **(C)** Steroid production in differentiated (d8) non-induced (-DOX-TMP) and induced (+DOX+TMP) cells stimulated for 24 h with vehicle (BSA), FSH, LH (0,100 ng/mL), or forskolin (10 μM). Each bar value represents mean ± SEM of technical replicates in a representative example of a total of 2 differentiation experiments. Medium contained minor amounts of progesterone. BSA, bovine serum albumin; d, day of differentiation; DOX, doxycycline hyclate; FSH, follicle stimulating hormone; LH, luteinizing hormone, TMP, trimethoprim.

(Fig. 2C). In contrast, non-induced cells responded to hormonal stimulation by producing merely progesterone at a low level, while stimulation with forskolin induced estradiol secretion (Fig. 2C). Moreover, in induced and non-induced cells, secretion of early fetal adrenal androgens dehydroepiandrosterone and dehydroepiandrosterone sulfate or later glucocorticoids cortisol, cortisone, or mineralocorticoid aldosterone, which are characteristic for function of the human adrenal glands, was not detected (Supplementary Table 2). The results indicate that steroidogenesis was induced by *NR5A1* activation in the gonadal-like cells, and that stimulation with FSH further increased the levels of secreted steroids. Moreover, the differentiated NR5A1-induced cells are heterogeneous consisting of subpopulations of steroidogenic and non-steroidogenic male gonadal-like cells.

2.3. NR5A1 induces multiple transcriptional changes

Principal component analysis with the entire transcriptome of the NR5A1-induced and non-induced sequenced samples on days 4, 6, 8, and 10 of differentiation indicated a clear divergence in transcriptional profiles between the conditions (Fig. 3A). We conducted pairwise DE comparisons of the samples between the treatment conditions at each specific time point, and within each treatment condition across time points as indicated in Fig. 3B (altogether 15 comparisons). On average, 8980 (range: 2691–15409) out of the total 60,619 genetic features (protein coding genes, non-protein coding genes *etc.*) assessed were detected to be differentially expressed per each comparison. Overall, a combined set of 22,692 genetic features showed differential expression from across the entire 15 analyses. The heatmap in Fig. 3 (Fig. 3C) presents the expression profiles of the top 20 DE genes detected from these analyses (adjusted $P<0.05$ using DESeq2, Love et al., 2014). While many of the genes present in the heatmap exhibited similar expression profiles independent of *NR5A1* activation, some clear differences can also be detected, indicating that *NR5A1* activation can cause major changes in the gene expression profile.

To evaluate the immediate effects of *NR5A1* expression, we performed more specific analyses comparing induced and non-induced cells on day 6 of differentiation (2 days after onset of induction). According to the pathway enrichment analysis performed using DAVID bioinformatics tools, genes upregulated ($\log_2FC\geq1$) in induced cells were primarily related to steroid synthesis, cholesterol metabolism, and male gonad development (Supplementary Fig. S3A, Supplementary Table 3). Genes downregulated ($\log_2FC\leq-1$) in induced cells were mainly associated with nervous system development and function and intracellular calcium ion balance. Due to the high number of upregulated DE genes at day 6 of differentiation, we decided to more specifically examine those that were within the top 100 significantly upregulated genes. Genes that are expressed during human fetal testis development and have previously been associated with steroidogenesis (such as *ACSS1*, *HPGD*, *GSTA1*, *C7*, *VCAM1*, *GRAMD1B* and *SERPINA5*, del Valle et al., 2017) were within the top 100 significantly upregulated genes ($\log_2FC>2$ in all) on day 6 of differentiation following *NR5A1* activation (Supplementary Fig. S3B, Supplementary Data 1). In addition, 51 of the top 100 upregulated genes were recognized to be associated with infertility, normal or abnormal gonadal development, or both using the curated Comparative Toxicogenomics Database (CTD) Gene-Disease Associations (Davis et al., 2009) and the curated GO Biological Process Annotations (Ashburner et al., 2000) datasets in the Harmonizome dataset collection (Rouillard et al., 2016). Within these top 100 upregulated genes, a NR5A1 target *MAMLD1* involved in spermatogenesis and the development of hypospadias and disorders of sex development was identified (Supplementary Fig. S3B, Supplementary Data 1, Fukami et al., 2006, 2008; Baxter et al., 2015; Miyado et al., 2017). In addition, a SC transcript ferritin receptor scavenger receptor class A member 5 (*SCARA5/TESR*, Sarraj et al., 2005; Jiang et al., 2006), *ITGAD/CD11d* (encoding an integrin alpha D subunit), and *ADAMTS14* (encoding a disintegrin and metalloproteinase), which to our knowledge have not previously been reported to be regulated by NR5A1, were recognized among the top 100 genes (Supplementary Fig. S3B, Supplementary Data 1). Likewise, *TDGF1/Cripto* encoding a co-receptor for Nodal and a ligand for src-Akt pathway signaling that modulates embryogenesis and tumorigenesis (Strizzi et al., 2005), was differentially expressed between the conditions (Supplementary Fig. S3B, Supplementary Data 1).

Within the top 100 significantly upregulated genes on subsequent days, *MAGEB1* (encoding a testis- and tumor-specific melanoma-associated antigen B1, Muscatelli et al., 1995; Lurquin et al., 1997) exhibited a delayed response to *NR5A1* activation by a nearly 200- and 100-fold increase in its expression on days 8 and 10 of differentiation, respectively, in the induced cells when compared with non-induced cells (Supplementary Data 1). To summarize, the sequencing data demonstrated that *NR5A1* activation induced several transcriptomic changes, including differential expression of known and putative gonad-associated genes.

2.4. NR5A1-induced cells presented dynamic gene-expression transcriptomics of various gonad-associated DE genes in a temporal manner

Next, NR5A1-induced DE genes presenting dynamic changes in their expression paths during the differentiation were identified by conducting time-series DE analyses using EBSeqHMM (Leng et al., 2015). Dynamic expression paths were grouped according to the direction of expression at each time point. For genes showing continuous upregulation (d4<d6<d8<d10), the path was labeled U–U–U. Accordingly, genes showing decreasing expression levels at each time point (d4>d6>d8>d10) were labeled D-D-D. A total of 215 genes categorized as U–U–U were associated with *e.g.* glutathione derivative biosynthesis, immune response, fatty acid and xenobiotic metabolism, ion transport, and oocyte development (Fig. 4A, Supplementary Table 4). A total of 144 genes upregulated on day 6 and stably expressed until day 10 of differentiation (U–S–S) were mainly linked to protein catabolism, dephosphorylation, cholesterol homeostasis, and steroid-hormone mediated signaling. In contrast, biological processes positively enriched among 216 genes whose expression was gradually repressed on days 6, 8, and 10 (D-D-D) included regulation of immunological response, glomerular development, and cell junction assembly, whereas 93 genes first downregulated between days 4 and 6 and stably expressed thereafter (D-S-S) were linked with intracellular calcium ion homeostasis. A total of 27 genes of the top 20 genes of each dynamic gene expression category (U–U–U, U–S–S, D-S-S and D-D-D, 80 genes in total, Fig. 4B), were associated with infertility, gonadal development, or both using the selected datasets in Harmonizome. Apart from a few genes participating in the structural integrity or function of male or female gonads (*TESC*, *HSD3B2*, *EMILIN1*, *CYP17A1*) (Rhéaume et al., 1991; Zhao et al., 1991; Perera et al., 2001; Bao et al., 2009; Yoshimoto and Auchus, 2015; Ouni et al., 2020) or RNA processing and apoptosis (*UTP11*, Heese et al., 2002, 2003), genes associated with infertility or gonadal development were not among the targets of NR5A1 in TRANSFAC Curated and Predicted Transcription Factor Targets datasets (Matys et al., 2003) in Harmonizome or the Ingenuity Pathway Analysis Knowledge Base (IPA). In addition to the genes associated with gonads, infertility, or both using Harmonizome datasets, other genes related to the gonads were recognized. For example, a ciliary function-associated *TTC21A* and *PLXNA1* encoding a semaphorin receptor were identified. *TTC21A* is expressed mainly in the testis and associated with sperm structure and function both in mice and humans (Liu et al., 2019) and *PLXNA1* is expressed within the developing sex chords of testes among other tissues in mice (Perälä et al., 2005). Neither of these were recognized as direct targets or interacting partners of NR5A1 using Harmonizome or IPA. In the category consisting of temporally downregulated genetic elements, *PCDH8* has been identified as a target of GC marker FOXL2 in murine primary follicular cells (Georges et al., 2014). Although PCDH8 was not recognized as a target of NR5A1 itself in

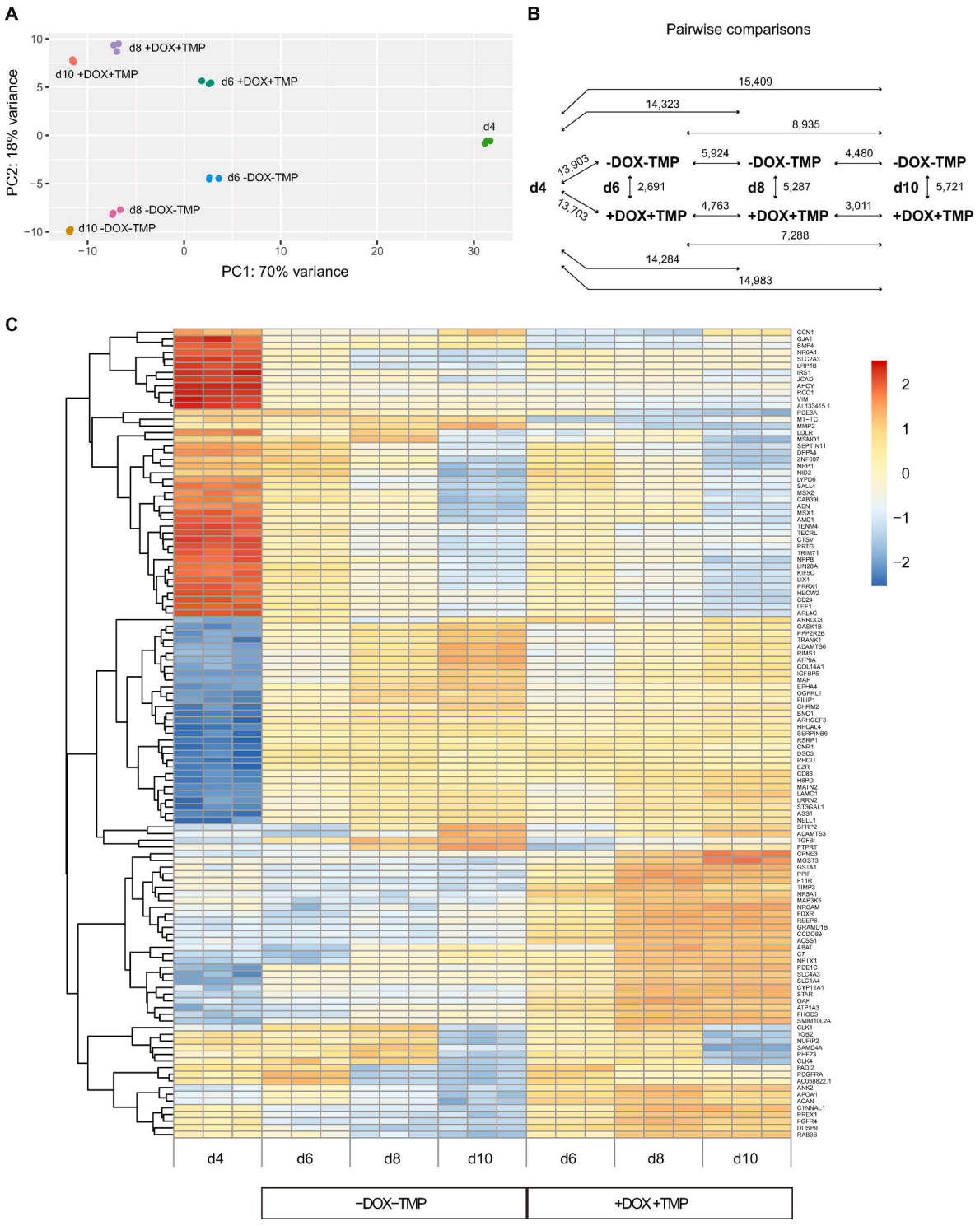

Fig. 3. NR5A1 drives differential gene expression transcriptomics in gonadal-like cells. **(A)** Principal component analysis for gene expression of RNA-sequenced induced (+DOX+TMP) and non-induced (-DOX-TMP) samples at differentiation days (d) 4, 6, 8, and 10. The scatter plot displays the position of samples based on the first two principal components (PCs). **(B)** A schematic diagram illustrating pairwise comparisons of sequenced samples using DESeq2. Each timepoint (d, day of differentiation) within a treatment condition (-DOX-TMP/+DOX+TMP) represents 3 technical replicates. The number of all differentially expressed genes in each pairwise comparison is shown. **(C)** Pairwise comparisons of RNA-sequenced non-induced (-DOX-TMP) and induced (+DOX+TMP) cell samples collected at differentiation days 4, 6, 8, and 10. The top 20 genes of each pairwise comparison are shown and the gene expression levels are scaled row-wise. The intensity of gene expression is indicated by a colour scale based on row z-scores (red, the highest expression levels; blue, the lowest expression levels). Each square represents a technical replicate. d, day; DOX, doxycycline hyclate; TMP, trimethoprim.

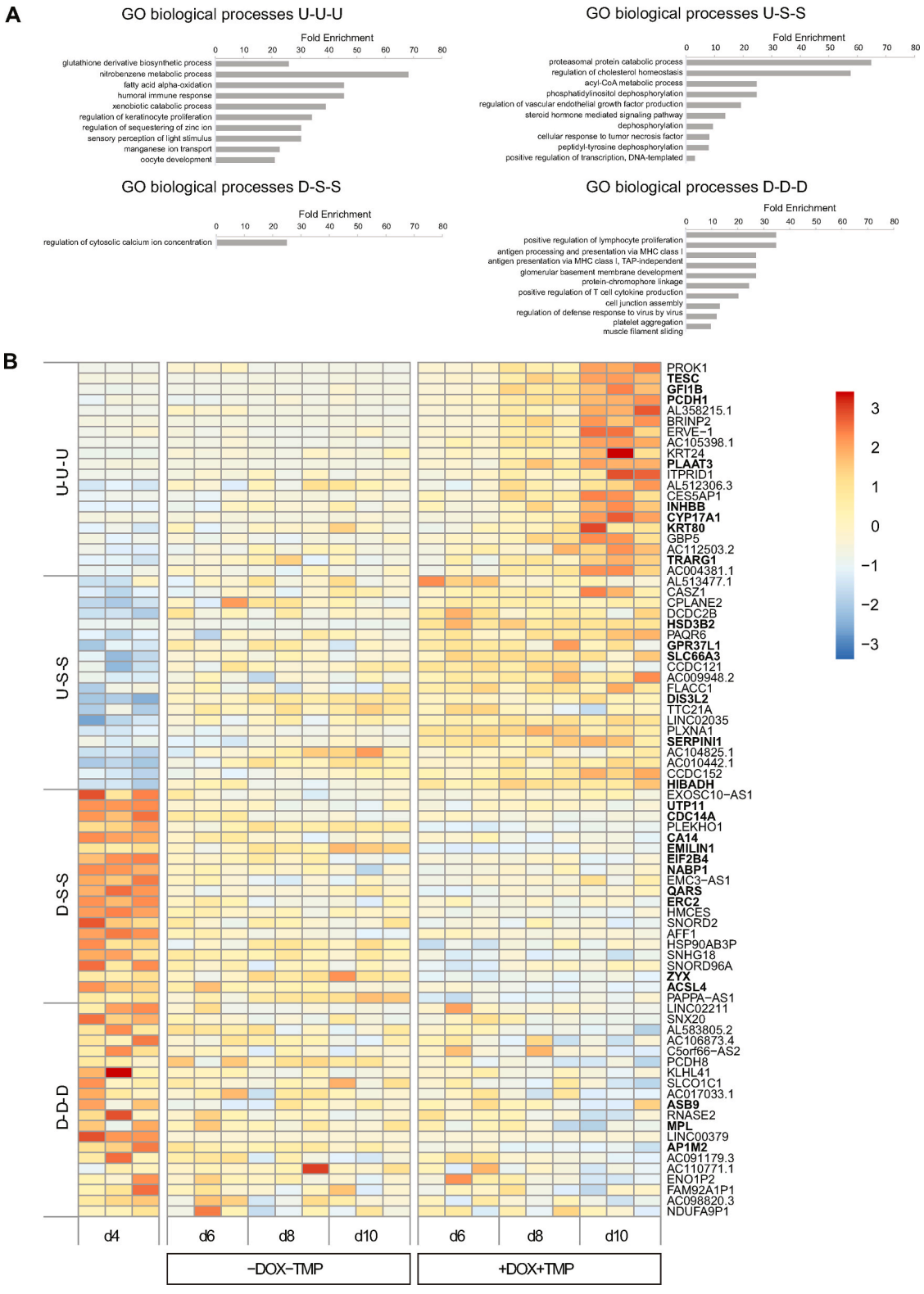

Fig. 4. NR5A1 induces dynamic changes in the expression of DE genes in developing male gonadal-like cells. **(A)** The top 10 GO biological process terms enriched within each dynamically differentially expressed category (U–U–U, U–S–S, D-S-S, D-D-D) in the NR5A1-induced condition. **(B)** Top 20 genes in each dynamic gene expression category indicating temporal expressional changes exclusively in the presence (+DOX+TMP) of *NR5A1* activation. Genes associated with infertility and/or gonadal development or function are bolded. U–U–U, gradual upregulation on days 6–10; U–S–S, upregulation on days 4–6 followed by stable expression thereafter; D-S-S, downregulation on days 4–6 and stable expression thereafter; D-D-D, gradual downregulation on days 6–10. The intensity of gene expression is indicated by a colour scale based on row z-scores (red, highest expression levels; blue, lowest expression levels). Each square represents a technical replicate. d, day of differentiation; DE, differentially expressed; DOX, doxycycline hyclate; TMP, trimethoprim.

Harmonizome or in the published literature, FOXL2 associates with NR5A1 in transcriptional regulation of several of its downstream targets (Park et al., 2010; Kashimada et al., 2011; Takasawa et al., 2014; Jin et al., 2016). Thus, various gonad-associated DE genes were dynamically expressed during the differentiation of gonadal-like cells.

2.5. Expression kinetics of candidate NR5A1 targets

Putative NR5A1 targets *SCARA5*, *MAGEB1*, *ADAMTS14*, *TDGF1*, and *ITGAD* were selected among the top 100 significantly upregulated genes and their expression kinetics were monitored in a time-course analysis, which included several time points starting from the onset of induction. *NR5A*1 was significantly upregulated 8 h after the beginning of induction (+DOX+TMP) (Mann Whitney *U* test, *P*=0.027, n=3) and the expression level increased further in the following time points. In non-induced (-DOX-TMP) cells, *NR5A1* expression remained at the basal level (Fig. 5A). Significant upregulation of a known NR5A1 target *CYP11A1* (Mann Whitney *U* test, P=0.0098, n=3), and a putative NR5A1 target *SCARA5* (Mann Whitney *U* test, *P*=4.3E-4, n=3) was detected 24 h after the onset of *NR5A1* activation (Fig. 5A). Similarly, expression of a predicted NR5A1 target in Harmonizome (*MAGEB1*), and other putative NR5A1 targets (*ADAMTS14*, *TDGF1*, and *ITGAD*) increased within 48 h after induction, with no or very low expression in its absence (Fig. 5A). Expression of testis-associated proteins SCARA5 and MAGEB1 was detected by positive immunolabeling at day 10 of differentiation in NR5A1-induced cells (Fig. 5B), in which the proteins were detected in both SF1-positive and -negative cells. Results from the expression analyses demonstrate a delayed but induced response to *NR5A1* activation by putative targets *SCARA5*, *MAGEB1*, *ADAMTS14*, *TDGF1*, and *ITGAD*.

3. Discussion

NR5A1 is elementary for the development of steroidogenic tissues and for the regulation of steroidogenic processes (Luo et al., 1994; Sadovsky et al., 1995; Morohashi and Omura, 1996). The effects of NR5A1 have previously been studied in gonadal-like cells differentiated from mouse ESCs (Jadhav and Jameson, 2011). In this study, we used a slightly similar approach, in which we generated steroid-producing and hormone-responsive early gonadal-like cells from male hiPSCs by combining directed differentiation and activation of the NR5A1 gene encoding SF1. In addition, we revealed that NR5A1 drives transcriptional and functional changes in bipotential gonadal-like cells and identified several NR5A1 candidate targets during their differentiation towards more mature gonadal cells with typical characteristics of male somatic cell types.

Based on public reference datasets our NR5A1-induced cells were annotated as somatic gonadal cells (SCs, LCs or GCs) and presented characteristics of immature SCs, derivatives of a common NR5A1-positive gonadal progenitor population (Stévant et al., 2018) and that can be generated *in vitro* via forced expression of *NR5A1* (Buganim et al., 2012; Liang et al., 2019; Rore et al., 2021). Following induction of NR5A1 expression, the differentiated cells in this study expressed and secreted AMH, a glycoprotein hormone specifically produced by immature testicular SCs (Tran et al., 1977; Rajpert-De Meyts et al., 1999). Increased NR5A1 expression also resulted in upregulation of inhibin α and SOX9, an early marker of SCs that is crucial for inducing testicular fate (Chaboissier et al., 2004). These results are consistent with previous studies performed with rodents demonstrating that NR5A1 controls the expression of AMH (Shen et al., 1994; Giuili et al., 1997; Watanabe et al., 2000), inhibin α (Ji et al., 2013), and SOX9 (Sekido and Lovell-Badge, 2008) in SCs.

According to our sequence analyses, male gonadal development was among the top 10 biological processes enriched in the NR5A1-induced cells at day 6 of differentiation. Also, NR5A1 is a known regulator of steroid hormone and cholesterol biosynthesis (Morohashi and Omura, 1996; Baba et al., 2018) and indeed, various genes or proteins acting on the steroidogenesis pathway and related to steroidogenesis in human fetal testes (such as STAR, CYP11A1, CYP17A1, HSD3B2, HSD17B3 and LHGCR, del Valle et al., 2017; Savchuk et al., 2019) were upregulated following *NR5A1* activation. Nr5a1 has previously been reported to upregulate steroidogenic genes in gonadal-like cells differentiated from mouse ES cells (Jadhav and Jameson, 2011). Further, in our study the activation of *NR5A1* expression induced secretion of progesterone, androstenedione, 17-OH progesterone and estrogens into culture media. The differentiated cells also expressed mRNA transcripts of the *FSHR*, which participates in FSH-stimulated proliferation of SCs in fetal rodents and in postnatal mice (Orth, 1984; Rannikko et al., 1995; Johnston et al., 2004; Migrenne et al., 2012). FSH, which induces steroid metabolism in immature SCs (Welsh and Wiebe, 1976; McDonald et al., 2006), was similarly able to increase the production of these steroidogenic hormones in our male gonadal-like cells. These data suggest that the differentiation protocol together with activation of *NR5A1* promotes differentiation of steroidogenic and hormone-responsive gonadal cells. The brief stepwise differentiation together with the detected expression of immature SC markers and lack of secreted testosterone suggests that the gonadal cells mimicked fetal rather than adult cells of testes. Although several typical characteristics of SCs were recognized, the exact identity of the differentiated NR5A1-induced cells remained ambiguous likely due to cell heterogeneity in the culture.

Furthermore, NR5A1 induced transcriptional changes in several genes with yet unknown or elusive association with NR5A1. A suggested NR5A1 target *MAGEB1* is localized in the dosage-sensitive sex reversal region and is expressed exclusively in testis and various tumors (Muscatelli et al., 1995; Lurquin et al., 1997) but its function is currently not well known. To our knowledge, no interaction between NR5A1 and MAGEB1 has previously been reported in any particular testicular or ovarian cell types. On top of that, we identified several other genes not previously linked to NR5A1 as its putative targets. *SCARA5* encodes a ferritin receptor that mediates non-transferrin-dependent delivery of iron in developing organs and participates in immune defense (Li et al., 2009). It is also involved in adipocyte commitment (Lee et al., 2017) and proliferation and progression of various cancer types (Huang et al., 2010; Liu et al., 2013; Wen et al., 2016; You et al., 2017). In fetal mice, *Scara5* can be first detected in gonads of both sexes but later becomes sex-dependently expressed (Sarraj et al., 2005). In adult mice, it is expressed in SCs and epithelial cells interacting with the mucosa (Sarraj et al., 2005; Jiang et al., 2006). *SCARA5* is furthermore associated with male infertility in the CTD Gene-Disease Associations dataset. In our study, SCARA5 expression was induced both at the transcriptional and protein levels exclusively in the presence of *NR5A1* activation with kinetics identical to that of *CYP11A1*, a known direct target of NR5A1, suggesting that NR5A1 directly regulates SCARA5 in developing gonads. The actual role of SCARA5 in male gonadal development remains to be elucidated. Another gene clearly upregulated by NR5A1 in our study was *TDGF1* which is expressed in male germ cells where it regulates male germ cell potency (Souquet et al., 2012; Spiller et al., 2012). Although not linked to development of testicular cells in previous studies, *TDGF1* is associated with urogenital abnormalities in the CTD Gene-Disease Associations dataset. The finding that NR5A1, either directly or indirectly, can regulate its expression suggests that TDGF1 may indeed be involved in the development of somatic cell lineages in testes.

ITGAD encodes integrin alpha-D (Wong et al., 1996), a member of the β2 integrin family of membrane glycoproteins, that is expressed on the surface of various types of leukocytes in human (Van der Vieren et al., 1995; Grayson et al., 1998; Siegers et al., 2017). This integrin mediates leukocyte cell adhesion and is linked to development of atherosclerosis and predisposition to diabetes (Grayson et al., 1998; Van der Vieren et al., 1999; Aziz et al., 2017; Cui et al., 2018). In addition, *ITGAD* is associated with urogenital abnormalities and female genital diseases in the CTD Gene-Disease Associations dataset. Another DE gene

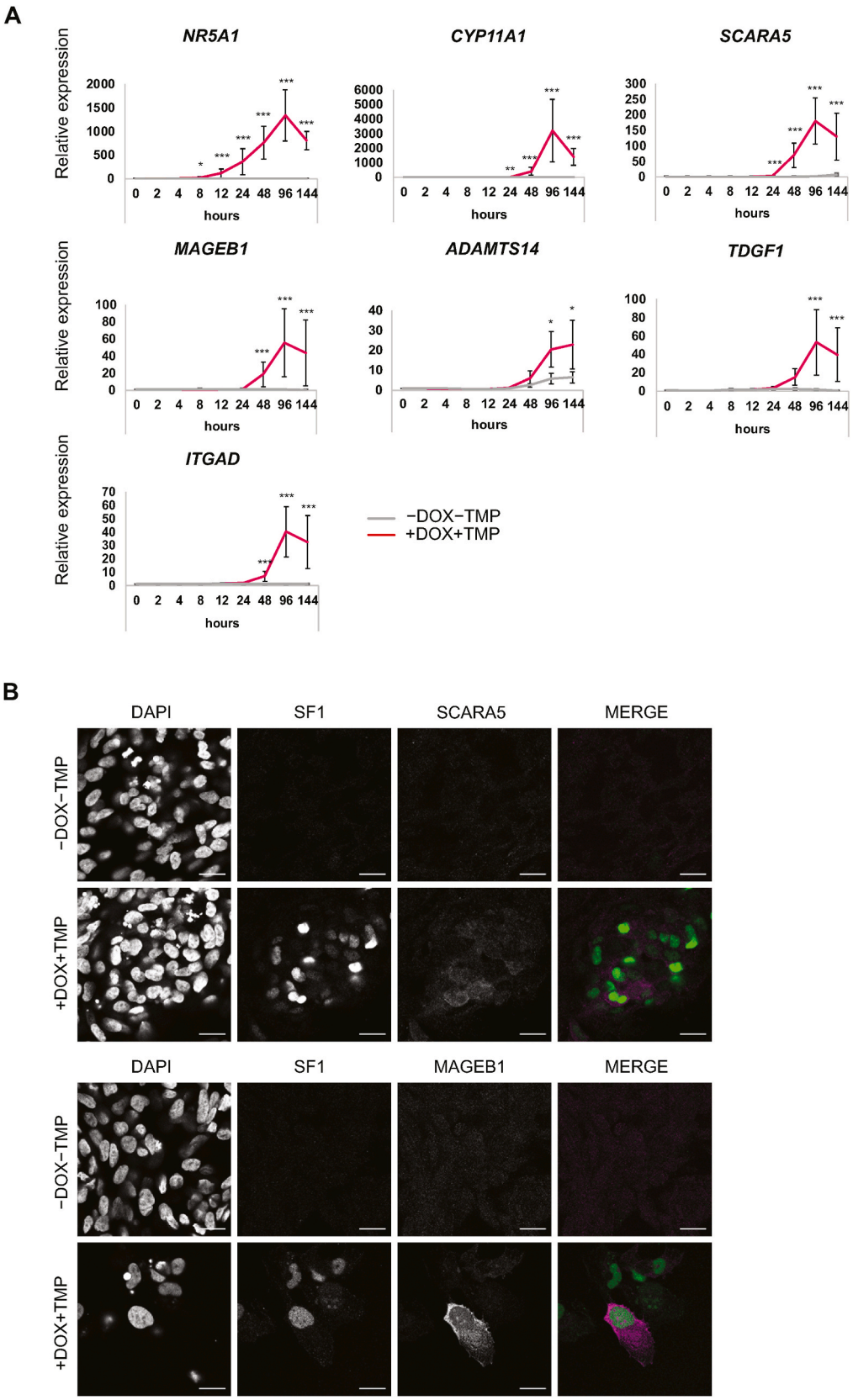

Fig. 5. NR5A1 regulates common and candidate targets in male gonadal-like cells. **(A)** Relative gene expression of pre-selected markers in the absence (-DOX-TMP) and presence (+DOX+TMP) of *NR5A1* activation. Each sample represents mean ± SEM (n=3–4). Expression levels are relative to gene expression before medium change at day 4 of differentiation (*$P<0.05$, **$P<0.01$, ***$P<0.001$, Mann Whitney *U* test with mean ranks). **(B)** Confocal microscopy of immunostained gonadal-like cells at day 10 of differentiation labeled against SCARA5 or MAGEB1. DAPI was used to stain cell nuclei. Individual channels were combined in merge with SF1 (green) and SCARA5/MAGEB1 (magenta). Images were taken from representative areas. Scale bars 20 μm. DOX, doxycycline hyclate; TMP, trimethoprim.

not previously associated with NR5A1 is *ADAMTS14*, which encodes a protease expressed in different trophoblast cells during gestation (Lee et al., 2014) and has previously been associated with certain types of cancer (Porter et al., 2004; De Robertis et al., 2018; Lin et al., 2020), multiple sclerosis (Goertsches et al., 2005), and osteoarthritis (Rodriguez-Lopez et al., 2009). *ADAMTS14* is differentially expressed between fetal and adult LCs, with a higher expression in fetal LCs (Lottrup et al., 2017). According to our data, expression of *ITGAD* and *ADAMTS14* is clearly induced by NR5A1, suggesting they might have early, yet unknown roles in the development of human gonadal cells.

By using GO Annotation and CTD gene-disease datasets, we identified several markers related to gonadal development, infertility, or both among the dynamically expressed genes. Furthermore, by using TRANSFAC Curated and Predicted Transcription Factor Targets datasets and IPA, we could also recognize genes with a known or predicted connection to NR5A1. Moreover, in addition to providing information about the temporal expression paths of the DE genes in the pairwise comparisons of NR5A1-induced and non-induced datasets by DESeq2 method, we identified genes such as the testis marker *INHBB*, which were not differentially expressed in these analyses but exhibited dynamically changing expression paths due to *NR5A1* activation.

TESC, encoding tescalcin, was one of the dynamically expressed genes upregulated upon *NR5A1* activation at each time point. *Tesc* is differentially expressed in the developing male and fetal gonads in mice and in chickens (Perera et al., 2001; Bao et al., 2009) and encodes an EF-hand Ca^{2+}-binding protein that regulates cytoplasmic pH via interaction with Na+/H+ exchanger type-1 (Mailänder et al., 2001; Li et al., 2003). Moreover, *TESC* is predicted to be a target of NR5A1 in Harmonizome. Of the genes constantly downregulated (D-D-D) that thus possibly counteract male gonadal development, *ASB9* and *MPL* are involved in folliculogenesis (Sarkar et al., 2011; Benoit et al., 2019). Of the genes first downregulated and then stably expressed at a lower level, *CDC14A* encodes a protein phosphatase that regulates oocyte maturation in mice (Schindler and Schultz, 2009) and is essential for spermatogenesis and male fertility both in mice and humans (Imtiaz et al., 2018; Wen et al., 2020), while *ACSL4* encodes an acyl-CoA synthetase required for steroidogenesis (Maciel et al., 2005). Neither of these genes are regulated by NR5A1 according to the TRANSFAC Curated and Predicted Transcription Factor Targets in Harmonizome or by the IPA. Furthermore, genes within this category included *EMILIN1*, which encodes the extracellular matrix component elastin microfibril interface-located protein 1 involved in elastogenesis (Zanetti et al., 2004) that can be found for instance in adult human ovaries (Ouni et al., 2020). Downregulation of *EMILIN1* in NR5A1-induced cells suggests suppression of the ovarian differentiation pathway in testicular-like cells.

Gonadotropins are critical regulators of gonadal steroidogenesis, gametogenesis and development of reproductive organs (O'Shaughnessy and Fowler, 2011; Ramaswamy and Weinbauer, 2015) and initiate different intracellular signaling cascades, of which the cAMP pathway can be targeted via activation of a guanine nucleotide binding protein (O'Shaughnessy and Fowler, 2011; Ramaswamy and Weinbauer, 2015; Casarini and Crépieux, 2019). Consistent with our results from FSH stimulation of the differentiated non-induced cells, previous studies have also revealed FSH-induced StAR (protein or mRNA) expression in cultured rat SCs (Gregory and DePhilip, 1998) and in the testes of hypogonadal mice (Sadate-Ngatchou et al., 2004). Moreover, FSH decreased the level of *FSHR* mRNA transcripts, which has previously been demonstrated *in vivo* and in *in vitro* testicular cultures (Maguire et al., 1997; Sadate-Ngatchou et al., 2004). In contrast, LH did not stimulate cAMP signaling or steroid production. Hence, although the number of transcripts for *LHCGR* (a gene encoding LH receptor) increased in response to *NR5A1* activation, the receptor did not respond to LH stimulation, which might be due to the low level of receptor expression.

In conclusion, in this study hormone-responsive steroidogenic male gonadal-like cells were generated from hiPSCs by combining directed differentiation and CRISPR-assisted gene activation. The method could be applied to examine the function of a specific gene at different temporal periods of human fetal gonadal development. The gene activation approach could be further extended for other developmental contexts beyond reproduction. Furthermore, we identified both new and common NR5A1 targets and delineated their transcriptional dynamics during early stages of gonadal differentiation, which can substantially benefit modeling of gonadal development in patients with disorders of sex development and infertility.

4. Materials and methods

4.1. HEL46.11 DDdCas9Vp192 hiPSCs

HEL46.11 cell line (46,XY, RRID:CVCL_UL37, kindly provided by the Biomedicum Stem Cell Center, University of Helsinki, Helsinki, Finland) was engineered to express a DDdCas9-VP192 construct under the control of a DOX-inducible promoter. To this end, we PCR cloned the fragment containing tight promoter-DDdCas9VP192-T2A-GFP-IRES-Neo from the plasmid PiggyBac-tight-DDdCas9VP192-T2A-GFP-IRES-Neo (RRID:Addgene_102889) into a destination vector containing homology arms to the AAVS1 locus. We also cloned a CAG-rtTA DOX-responsive transactivator into a destination vector containing homology arms to the AAVS1 locus. We then electroporated HEL46.11 cells with the two plasmids described above together with eSpCas9(1.1)_No_FLAG_AAVS1_T2 (RRID:Addgene_79888), to introduce strand breaks at the AAVS1 locus and stimulate homologous recombination of both donor plasmids. After expansion and selection with G418 (Thermo Fisher) for 2 weeks, resistant clones were treated with DOX to test the induction of DDdCas9-VP192-GFP construct. Functional GFP-expressing clones were further single-cell cloned as described below to obtain a clonal DDdCasVP192-GFP inducible cell line (clone 3H/G4) that was used in subsequent experiments.

4.2. Guide RNA design and production

Guide RNA sequences were designed using a free web-based research platform (Benchling, RRID:SCR_013955, https://benchling.com, Benchling Inc., San Francisco, CA) by targeting them to the proximal promoter region (−350 to −50 bp from transcription start site) of the NR5A1 gene. Guides were selected based on their target efficiency scores and position. To test their ability to induce *NR5A1*/SF1 expression, each guide was incorporated into guide RNA transcriptional units as previously described (Balboa et al., 2015). Briefly, guide RNA sequences, U6 promoter, and terminator products amplified from pX335 were combined by PCR with Phusion High-Fidelity DNA polymerase (ThermoFisher, Vilnius, Lithuania). Each PCR reaction of 100 µL total volume contained 50 pmol forward (Fw) and reverse (Rv) primers, 2 pmol guide oligo, 5 ng U6 promoter and 5 ng terminator PCR products. PCR program parameters were 98°C/3 min, 98°C/10 s, 52°C/30 s, and 72°C/12 s for 35 cycles. Guide RNA-PCR products were purified with NucleoSpin Gel and PCR Clean-up kit (Macherey Nagel, Düren, Germany) and tested alone and in various combinations in HEK293 cells (RRID:CVCL_0045, ATCC line CRL-1573, kindly provided by the Biomedicum Stem Cell Center). Four guide-PCR products selected based on their activity to induce *NR5A1*/SF1 expression were concatenated with Golden Gate Assembly (Cermak et al., 2011) into a GG-dest vector (RRID:Addgene_69538, Balboa et al., 2015). Guide assembly reactions, transformation of the reaction products into DH5α chemically competent bacteria (New England Biolabs, Inc.), and screening of positive colonies was performed as previously described (Balboa et al., 2015). Successful concatenation of the guide-PCR products was confirmed by Sanger sequencing at Eurofins Genomics, Köln, Germany. Subsequently, concatenated guides were subcloned into a PiggyBac plasmid (RRID: Addgene_102893, plasmid without the insert, Addgene) via Epstein-Barr

virus nuclear antigen plasmid (RRID:Addgene_102898, plasmid without the insert, Addgene, both kindly provided by the Biomedicum Stem Cell Center, Weltner et al., 2018).

4.3. Cell transfection for testing guide transcriptional units

HEK293 cells were seeded at a density of 10^5 cells/well on gelatin-coated 24-well plates 1 day prior to transfection. Cells were transfected with FUGENE® HD Transfection Reagent (Promega Corporation, Madison, WI, USA) in high-glucose DMEM supplemented with GlutaMAX™ (Gibco™) + 10% fetal bovine serum (FBS, Gibco™) using 500 ng of CAG-dCAS9-VP192-T2A-EGFP-ires-puro transactivating domain encoding plasmid (Balboa et al., 2015) and 200 ng of guide-transcriptional unit. For testing combinations of guide transcriptional units in *NR5A1* activation, a pool consisting of 200 ng of guide-PCR products was transfected. Guide-PCR testing was performed in triplicate wells. Samples for qPCR and immunocytochemistry were collected 72 h post-transfection. The induced expression of *NR5A1* by dCas9 targeted by selected guides in HEK293 cells is shown in Supplementary Fig. 4A.

guide RNA oligos.

gNR5A1_3:GTGGAAAGGACGAAACACCGGAGGCCTGCA-GAGTCACGTGGTTTTAGAGCTAGAAATAG
gNR5A1_7:GTGGAAAGGACGAAACACCGAGGCCTGCA-GAGTCACGTGGGTTTTAGAGCTAGAAATAG
gNR5A1_9:GTGGAAAGGACGAAACACCGCACCCGGTTTCTAA-CAAGCGGTTTTAGAGCTAGAAATAG
gNR5A1_11:GTGGAAAGGACGAAA-CACCGCAGGGAGGTAGCCATTCACAGTTTTAGAGCTAGAAATAG

Sequences for Golden Gate concatenation.

1_aggc_Fw ACTGAATTCGGATCCTCGAGCGTCTCACCCTGTAAAAC-GACGGCCAGT
1_aggc_Rv CATGCGGCCGCGTCGACAGATCTCGTCTCACATGAGGA AACAGCTATGACCATG
2_aggc_Fw ACTGAATTCGGATCCTCGAGCGTCTCACATGGTAAAAC GACGGCCAGT
2_aggc_Rv CATGCGGCCGCGTCGACAGATCTCGTCTCAGTCCAGGA AACAGCTATGACCATG
3_aggc_Fw ACTGAATTCGGATCCTCGAGCGTCTCAGGACGTAAAAC-GACGGCCAGT
3_aggc_Rv CATGCGGCCGCGTCGACAGATCTCGTCTCACTGGAGGA AACAGCTATGACCATG
4_aggc_Fw ACTGAATTCGGATCCTCGAGCGTCTCACCAGGTAAAAC-GACGGCCAGT
5_aggc_Rv CATGCGGCCGCGTCGACAGATCTCGTCTCACGTTAGGAA ACAGCTATGACCATG

4.4. Cell electroporation

PiggyBac plasmid containing four guides targeting *NR5A1* promoter (Supplementary Fig. 4B) was introduced into HEL46.11 DDdCas9Vp192 hiPSCs (kindly provided by Dr. Diego Balboa, Biomedicum Stem Cell Center) with Neon™ Transfection System (Invitrogen). Cells were cultured until 80% confluence and incubated in Y-27632 2HCl (Selleckchem, Houston, Texas, USA) 4 h prior to electroporation. Cells were dissociated with StemPro® Accutase® (Gibco, Grand Island, NY, USA) and suspended in cold 5% FBS-PBS (PBS, phosphate-buffered saline). Shortly before electroporation, cells were counted and resuspended in R buffer (Invitrogen, CA, USA) at a density 2 x 10^6 cells/mL. The following program parameters were used for cell transfection: 1100 V, 20 ms, 2 pulses. Transfected cells were incubated on Geltrex® LDEV-Free human embryonic stem cell-qualified Reduced Growth Factor Basement Membrane Matrix (Gibco, Thermo Fisher Scientific, Waltham, MA, USA) -coated dishes 24 h prior to first medium change. Selection for colonies containing guides targeting *NR5A1* promoter (HEL46.11 DDdCas9Vp192-NR5A1 hiPSCs) was started 72 h after transfection with 5 μg/mL puromycin (Gibco, Grand Island, NY, USA) for 2 days followed by 2.5 μg/mL puromycin for 4 additional days.

4.5. Generating clonal lines

HEL46.11 DDdCas9Vp192-NR5A1 hiPSCs were incubated with 10 μM Y-27632 2HCl (Selleckhem, Houston, Texas, USA) in Essential 8™ (E8) Basal Medium (Thermo Fisher Scientific, MA, USA) for at least 4 h prior to dissociation with StemPro® Accutase® (Gibco™, Thermo Fisher Scientific). Dissociated cells were resuspended in 10% FBS (Thermo Fisher Scientific) in PBS and centrifuged at 17×*g* for 3 min. The cell pellet was resuspended in FACS buffer containing Hank's Balanced Salt Solution (Gibco™, Thermo Fisher Scientific, NY, USA), 1 mM Ultrapure™ EDTA (Invitrogen™, Thermo Fisher Scientific, NY, USA), 25 mM HEPES (Lonza™, Fisher Scientific, MD, USA), 10% FBS, and 10 μM Y-27632. Cells were passed through a Cell Strainer (40 μm, FALCON™, Thermo Fisher Scientific), counted with Countess II Automated Cell Counter and kept on ice until sorting according to their size and singularity into 96-well plates containing E8, 5 μM Y-27632, Penicillin Streptomycin (Gibco™, Thermo Fisher Scientific), and Clone R™ (STEMCELL Technologies, Canada). Cell sorting was performed with SH800Z Cell Sorter (SONY). After sorting, plates were centrifuged at 17×*g* for 3 min and incubated at 37°C. Half of the medium was changed 2 days after sorting and colonies were cultured in E8 until they could be picked and expanded.

4.6. Cell culture

All cells were cultured in a humidified incubator supplied with 5% CO_2 at 37°C and tested negative for mycoplasma contamination. HEL46.11 DDdCas9Vp192-NR5A1 hiPSCs were cultured on Geltrex® -coated Tissue-Culture Treated Dishes (Corning, NY USA) in Essential 8™ medium (Thermo Fisher Scientific, Grand Island, NY, USA) and routinely passaged every 3–4 days. For cell passaging, 0.5 mM EDTA (Invitrogen™, Thermo Fisher Scientific, Grand Island, NY, USA) in PBS was incubated on cells for 3–4 min. Differentiation was performed as described in our earlier study (condition M, Sepponen et al., 2017). Similar differentiation outcome and activation of *NR5A1* was confirmed both in the unsorted pool of cells and in the clone 14, which was used in all experiments. Cells were differentiated in 3 replicate wells for steroid, AMH immunoassay and RNA sequencing analyses and in at least 2 replicate wells for qRT-PCR and cAMP immunoassay analyses. Undifferentiated hiPSCs were dissociated with EDTA, counted, and seeded at density 1.5 x $10^5/cm^2$ on Tissue-Culture Treated 12-well cell culture plates (Corning, Kennebunk, ME, USA) for collection of RNA or media and on polymer-coated μ-slide 4 wells (ibidi GmbH, Gräfelding, Germany) for immunofluorescent antibody labeling. Due to inconsistent availability of the product, Human Type I collagen from two different sources was used for coating the 12-well cell culture plates in the differentiation studies. All experiments, including hormonal stimulation, were performed using human fibroblast-derived collagen (Stem Cell Technologies, USA). For the RNA sequencing experiment and most of the other gene and protein expression studies, coating was performed with human placental-derived collagen (Corning, NY, USA). Cells to be seeded were collected at 70×*g* for 5 min before resuspending into DMEM/F12 + Glutamax supplemented with 2% B27™ Supplement (Thermo Fisher Scientific). The medium additionally contained 10 μM Rho kinase inhibitor (Y-27632 2HCl, Selleckchem, Houston, Texas, USA), 100 ng/mL Activin A (Q-kine, Cambridge, UK), 5 μM GSK-3α/β inhibitor CHIR-99021, and BMP inhibitor dorsomorphin (both from Selleckchem) at 2 μM concentration. On the following day, the medium was replaced by differentiation medium containing 3 μM CHIR-99021 and 10 ng/mL BMP7 (Peprotech, Cranbury, NJ, USA). After 24 h,

conditioned medium was replaced with differentiation medium containing 3 μM CHIR-99021 and 2 μM dorsomorphin. Cells were washed once with PBS between medium replacements. To induce NR5A1 expression, cells were treated with 10 μg/mL doxycycline hyclate (DOX) and 10 μM trimethoprim (TMP, both from Sigma-Aldrich, Israel) in DMEM/F12 + Glutamax supplemented with 2% B27™ Supplement on days 4–10. Most of the conditioned medium was changed daily.

HEK293 cells were maintained on tissue culture-treated dishes in high-glucose DMEM supplemented with GlutaMAX™ (Gibco™) and 10% FBS. Cells were passaged every 2–4 days using Trypsin-EDTA (Thermo Fisher Scientific).

4.7. Immunofluorescence and confocal microscopy

At day 10 of differentiation, cells differentiated on the ibidi slides were fixed with 4% paraformaldehyde at room temperature for 20 min and washed three times with PBS. Cells were permeabilized with 0.5% Triton® X-100 (Fisher Scientific, NJ, USA) for 8 min and washed three times with PBS before antigen blocking with UltraVision Protein Block (Thermo Fisher Scientific, Kalamazoo, MI, USA) for 10 min. Cells were incubated with primary antibodies: monoclonal mouse anti-SF1 (R&D Systems Cat# PP-N1665-00, clone N1665, RRID:AB_2251509, 1:250), polyclonal rabbit anti-AMH (Abcam Cat# ab84415, RRID:AB_1860886, 1:200), monoclonal mouse anti-inhibin α (20/32, N-terminal, 26 μg/mL, Ansh Labs, Webster, TX, USA, kindly provided by Dr. Ajay Kumar), monoclonal rabbit anti-StAR (Cell Signaling Technology Cat# 8449, RRID:AB_10889737, D10H12, 1:100), polyclonal rabbit anti-P450SCC (Sigma-Aldrich Cat# HPA016436, RRID:AB_1847423, St. Louis, MO, USA, 1:200), polyclonal goat anti-GATA4 (Santa Cruz Biotechnology Cat# sc-1237, RRID:AB_2108747, C-20, 1:250), monoclonal mouse anti-HSD3B2 (Sigma-Aldrich Cat# SAB1402232, RRID:AB_10641572, St. Louis, MO, USA, clone 1E8, 1:100), polyclonal rabbit anti-SCARA5 (Sigma-Aldrich Cat# HPA024661, RRID:AB_1853902, St. Louis, MO, USA, 1:100), polyclonal rabbit anti-MAGEB1 (Novus Cat# NBP1-85405, RRID:AB_11034576, 1:100), or polyclonal goat anti-SOX9 (R&D Systems, Cat# AF3075, RRID:AB_2194160, 1:200). All primary antibodies were incubated on cells overnight at 4°C and subsequently removed by washing the samples three times with PBS. Alexa Fluor® 488 donkey anti-mouse immunoglobulin G (IgG) (Molecular Probes Cat# A-21202, RRID:AB_141607), Alexa Fluor® 594 donkey anti-goat IgG (Thermo Fisher Scientific Cat# A-11058, RRID:AB_2534105), or Alexa Fluor® 594 donkey anti-rabbit IgG (Molecular Probes Cat# A-21207, RRID: AB_141637) (all from Invitrogen, Life Technologies, OR, USA, 1:1000) secondary antibodies were incubated on cells for 30 min in the dark. Triple costainings were performed similarly with Alexa Fluor® 488 donkey anti-goat IgG (Molecular Probes Cat# A-11055, RRID: AB_2534102), Alexa Fluor® 647 donkey anti-mouse IgG (Molecular Probes Cat# A-31571, RRID:AB_162542), and Alexa Fluor® 568 goat anti-rabbit IgG (Molecular Probes Cat# A-11011, RRID:AB_143157) secondary antibodies (all from Invitrogen, Life Technologies, OR, USA, 1:1000). The samples were subsequently washed as above. All antibodies were diluted in 0.1% Tween (Fisher Scientific, NJ, USA) in PBS. Nuclei were labeled with 4′,6-diamidino-2-phenylindole (DAPI) Dilactate (Invitrogen, #D3571) at a 1:1000 ratio in PBS for 8 min in the dark and washed twice with PBS. Images were captured with a TCS SP8 laser scanning confocal microscope using a 1024x1024 scan format and a HC PL APO CS2 40x/1.10NA water objective (Leica Microsystems, Mannheim, Germany). Images were processed using Fiji ImageJ (version 1.53, http://fiji.sc). Image smoothing in Fiji was performed using a Gaussian filter with one pixel kernel radius. Image size was adjusted with Adobe Photoshop (version 23.0.0, Adobe, San Jose, CA, USA). The number of cells positive for SF1 per condition was manually counted from 7 original size zoom out images from representative areas, and the number of SOX9 and/or P450SCC positive cells from 2 to 4 images per condition.

4.8. Real-time qRT-PCR

Methods for RNA isolation, reverse transcription reaction, and qRT-PCR have been previously described (Sepponen et al., 2017). Primer sequences used for qRT-PCR are listed in Supplementary Table 5.

Briefly, total RNA was isolated, residual genomic DNA was removed in a separate step, and samples were purified prior to their conversion into complementary DNA with Moloney murine leukemia virus reverse transcriptase (Promega), random hexamer primers, oligo(dt)18 primers, RiboLock RNAse Inhibitor, and a mixture of four deoxynucleotide triphosphates (all from Thermo Fisher Scientific). After combining HOT FIREPol EvaGreen qPCR Mix Plus (Solis Biodyne, Tartu, Estonia) with cDNA and forward and reverse primers (Metabion, Planegg/Steinkirchen, Germany), the relative mRNA expression levels were analyzed with a Lightcycler® 96 system (Roche Diagnostics, Mannheim, Germany). The ΔΔCt method (Livak and Schmittgen, 2001) was followed for quantification of gene expression. Expression levels were normalized with cyclophilin G (*PPIG*) serving as an endogenous control and presented as relative to expression levels in undifferentiated cells.

4.9. Functional studies

For hormonal stimulations, differentiated cells at day 8 were washed once with PBS and incubated for 1, 8, or 24 h with human recombinant FSH (Prospec, Rehovot, Israel) or LH alpha/beta Heterodimer Protein (R&D Systems) at a concentration of 100 ng/mL, vehicle [0.1% bovine serum albumin (Thermo Fisher Scientific) in H_2O] or 10 μM forskolin (Sigma-Aldrich, St.Louis, MO, USA) in differentiation medium. Forskolin was used to activate adenylyl cyclase independently of receptor signaling. Intracellular cAMP was measured from cell lysates harvested from duplicate wells after 1-h stimulation with Direct cAMP ELISA kit (Enzo Life Sciences AG, Lausen, Switzerland, Cat# ADI-900-066) following the manufacturer's instructions. Optical density was read at 405 nm using a Multiscan EX Version 1.1 (type 355, Labsystems, Vantaa, Finland) microplate reader and the standard curve was prepared using Point-to-Point method. Gene-expression levels in samples incubated for 8 h in the presence/absence of gonadotropins were assayed by qRT-PCR. The production of steroids after 24-h stimulation with or without FSH/LH/forskolin was assayed from cell supernatants in triplicate wells with an established method applying liquid chromatography tandem-mass spectrometry (Ohlsson et al., 2021) at the Department of Internal Medicine and Clinical Nutrition, University of Gothenburg, Gothenburg, Sweden. Measured steroids included androstenedione (lower limit of quantification, LLOQ=0.018 nmol/L), dehydroepiandrosterone (LLOQ=0.87 nmol/L), dihydrotestosterone (LLOQ=44.8 pmol/L), estradiol (LLOQ=1.84 pmol/L), estrone (LLOQ=1.85 pmol/L), progesterone (LLOQ=0.016 nmol/L), 17-OH progesterone (LLOQ=0.060 nmol/L), and testosterone (LLOQ=0.017 nmol/L). LLOQ values provided are those obtained using human serum as the analysis matrix and LLOQ was defined as the lowest peak that was reproducible with a coefficient of variation of less than 20% and an accuracy of 80%–120%. Similar results were obtained using an independent liquid chromatography tandem-mass spectrometry analysis at the Department of Clinical Science, University of Bergen, Bergen, Norway using a method previously described (Triebner et al., 2014) and subsequently updated to include steroids typically produced by the adrenal glands. Analytical sensitivity and precision were determined as LLOQs and coefficient of variation for intermediate concentrations, respectively, for dehydroepiandrosterone sulfate (0.021 μmol/L and 10.4%), cortisol (0.59 nmol/L and 4.0%), cortisone (0.17 nmol/L and 4.2%), and aldosterone (13 pmol/L and 7.5%). Accuracies for the steroids measured at University of Bergen were in the range of 95–109%. Basal medium (DMEM/F12 with Glutamax+2% B27) used for cell differentiation served as a blank in the steroid assays.

Spent medium was collected and analyzed from duplicate culture wells with picoAMH ELISA (Ansh Labs, Webster, TX, USA, Cat# AL-124-

i) from cells differentiated until day 10. The absorbance was read using a Multiscan EX Version 1.1 (type 355, Labsystems) microplate reader set to 450 nm and 620 nm (machine blank) and the standard curve was prepared using Point-to-Point method.

4.10. RNA sequencing

Cells cultured in three wells/condition at differentiation days 4, 6, 8, and 10 were disrupted with QlAzol Lysis Reagent (Qiagen, MD, USA) directly on wells of tissue culture plates and collected. Total RNA was extracted and purified with miRNeasy Mini Kit (Qiagen, Hilden, Germany) including an additional On-Column DNase Digestion with the RNase-Free DNase Set. RNA quality monitoring, library preparation, and sequencing were performed by the Sequencing unit of Institute for Molecular Medicine Finland FIMM Technology Centre, University of Helsinki, Finland. RNA quality was confirmed with Bioanalyzer RNA Quality Control Assay and RNA libraries were prepared with TruSeq Stranded Total with Ribo-depletion. Sequencing was performed with an Illumina NovaSeq system using an S4 flow cell with lane divider (Illumina, San Diego, CA, USA). Read length for the paired-end run was 151+8+8+151 bp and the target sequencing depth was 25 million read pairs. Two rounds of sequencing were performed for samples that did not meet the target depth level and the resulting read files were merged for running feature counting.

Data pre-processing was performed at FIMM. Quality control of raw sequence data was conducted with FastQC-0.11.5. Reads were trimmed and filtered with Trimmomatic-0.32. Reads were then aligned against the human genome (GRCh38 release 82) using STAR 2.3.0e. RNASeq quality was assessed with picard-tools-1.119. RNA-SeQC v1.1.8. "Gene-level" read counting using Ensembl gene-ids was generated by featureCounts software (Subread-1.4.5-p1) resulting in genome-wide quantification of reads aligning to all genetic features, including both protein coding and non-coding features (such as long non-coding RNAs).

4.11. Data analysis

The gene-level RNAseq quantification data from all samples was combined into one gene-by-sample expression data matrix for pairwise DE analyses with DESeq2 (v1.24, Love et al., 2014), and ordered time-series dynamic DE analyses with EBSeq-HMM (v1.18, Leng et al., 2015).

R package scCATCH (version 3.0; https://github.com/ZJUFanLab/scCATCH, Shao et al., 2020) was used to annotate sample clusters (*i.e.* samples at each time point compared to samples in all other time points) to cell types using reference tissues related to gonad. A score of similarity was calculated after sample-cluster specific markers with logFC≥1 were detected with the findmarkergene function in scCATCH.

For the analyses with DESeq2 (Fig. 3C), pairwise comparisons were conducted between the induced and non-induced samples at each time point (d6, d8, d10), and between samples from the same condition (induced, or non-induced) but from different time points, altogether making 15 analyses (Fig. 3B). All genes/features with an adjusted $P<0.05$ were considered significantly differentially expressed. For the time-series DE analyses by EBSeqHMM, samples in the NR5A1-induced condition were analyzed by specifying the time-points (d4, d6, d8, d10) as the ordering condition of the samples. For all genes, EBSeqHMM estimates posterior probabilities (PP) for all likely paths of gene expression changes across the ordered time condition (upregulation at each time point, U–U–U, downregulation at each time point D-D-D, *etc.* for 3^3=27 possible paths for each gene; possible changes at each transition are U for upregulated, D for downregulated, and S for unchanged stable expression). Genes showing significant differential expression in at least one time point (compared to an earlier time point), and genes with PP<0.05 of remaining constant, under an overall target FDR<0.05, were called DE genes. The DE genes were assigned the path for which they showed highest PP (MaxPP), and were divided into clusters of genes based on the dynamic gene expression path they followed. The subsequent analyses considered selected paths, which presented the immediate (U–S–S, D-S-S) and continued (U–U–U, D-D-D) dynamic responses to *NR5A1* activation.

Default normalization and statistical methods implemented in both DESeq2 and EBSeqHMM were used for all analyses. For the visualization of the expression dataset with principal component analysis, variance stabilized data from DESeq2 was used.

4.12. GO enrichment analyses for sequencing data

All GO enrichment analyses were performed using DAVID Functional Annotation Tool (DAVID, RRID:SCR_001881, v6.8, https://david.ncifcrf.gov/, Huang et al., 2009a; 2009b). The gene expression matrix derived from RNA sequencing was normalized and log2-transformed, and after removal of genes without any detected transcripts it was used as a reference gene set in all GO enrichment analyzes. Pre-filtered genes within d6 pairwise compared samples (Supplementary Data 1; Upregulated $\log_2FC\geq1$ or Downregulated $\log_2FC\leq-1$ and adjusted $P<0.05$) and all genes within each category of dynamically expressed genes (Supplementary Data 2; U–U–U, U–S–S, D-S-S, or D-D-D) were used as input genes. The output GO biological processes were sorted according to the false discovery rate and fold enrichment values.

Genes related to male or female infertility or gonadal development were searched among all dynamically expressed genes within four categories (U–U–U, U–S–S, D-S-S, and D-D-D) within the curated CTD Gene-Disease Associations (Davis et al., 2009) and the curated GO Biological Process Annotations (Ashburner et al., 2000) datasets using Harmonizome (Harmonizome, RRID:SCR_016176, http://amp.pharm.mssm.edu/Harmonizome/, Rouillard et al., 2016). A search for identifying known or predicted targets or interaction partners of *NR5A1* was performed using TRANSFAC Curated and Predicted Transcription Factor Targets datasets (Matys et al., 2003) using Harmonizome and the IPA software (Ingenuity Pathway Analysis, RRID:SCR_008653, v68752261, Qiagen, http://www.ingenuity.com/products/pathways_analysis.html).

4.13. Statistical analyses

When used, "n" indicates the number of independent experiments. Statistical analyses for data derived from qRT-PCR, AMH immunoassay analyses, or cell counts were conducted with IBM SPSS Statistics 25 software by performing pairwise comparisons using Mann Whitney *U* test with mean ranks or independent samples *t*-test according to the sample set. Shapiro-Wilk test was used to assess normal distribution. Benjamini and Hochberg method was used to adjust *P*-values in pairwise comparisons of the gene expression data obtained from RNA sequencing and qRT-PCR. In case of multiple groups, one-way ANOVA using Dunnett *t*-tests (2-sided) as post-hoc tests were performed. $P<0.05$ was considered to indicate statistical significance. All statistical analyses were performed at confidence level 95%.

Author contributions

Conceptualization: KSe, KL, TT, and JST; Methodology: KSe, DAY, SV, DB, OR, MP, CO, SH, EB, PP, KL, TT, and JST; Investigation: KSe, DAY, SV, and EB; Resources: DB, TO, OR, CO, and SH; Data processing, curation and visualization: KSe and DAY; Writing –original draft: KSe; Manuscript revision and editing: KSe, KL, TT, JST, OR, DAY, DB, SV, PP, MP, CO, TO, SH, EB, and KSa; Supervision: KL, TT, and JST; Funding acquisition: KL, TT, and JST; Project administration: KSe.

Funding

This work was supported by the Sigrid Jusélius Foundation, the Academy of Finland (Grant 295760), Helsinki University Hospital

Funds, and the Novo Nordisk Foundation (Grant 10825).

Data and material availability

RNA sequencing raw and processed read files have been deposited in NCBI's Gene Expression Omnibus and can be accessed through GEO Series accession number GSE186606. All material unique to this study is available from the corresponding author upon request.

Declaration of competing interest

none.

Acknowledgements

The authors thank Dr. Jere Weltner for valuable advice on concatenation and subcloning of NR5A1 guide RNAs and Solja Eurola for advice in production of guide RNA transcriptional units. We thank professor Jorma Toppari at the University of Turku for valuable comments on fetal testicular steroidogenesis. Dr. Ajay Kumar (Ansh Labs, Webster, Texas, USA) is kindly thanked for the inhibin α subunit monoclonal antibody used in this study. The FIMM NGS Unit of Institute for Molecular Medicine Finland FIMM Technology Centre at the University of Helsinki (supported by Biocenter Finland) and the Biomedicum Imaging Unit (HiLIFE) and the Biomedicum Flow Cytometry Unit (HiLIFE) at the University of Helsinki, Finland are acknowledged for skilled assistance with their services.

Appendix A. Supplementary data

Supplementary data to this article can be found online at https://doi.org/10.1016/j.diff.2022.08.001.

References

Achermann, J.C., Ito, M., Ito, M., Hindmarsh, P.C., Jameson, J.L., 1999. A mutation in the gene encoding steroidogenic factor-1 causes XY sex reversal and adrenal failure in humans [1]. Nat. Genet. 22, 125–126. https://doi.org/10.1038/9629.

Almeida, M.Q., Soares, I.C., Ribeiro, T.C., Fragoso, M.C.B.V., Marins, L.V., Wakamatsu, A., et al., 2010. Steroidogenic factor 1 overexpression and gene amplification are more frequent in adrenocortical tumors from children than from adults. J. Clin. Endocrinol. Metab. 95, 1458–1462. https://doi.org/10.1210/JC.2009-2040.

Anamthathmakula, P., Miryala, C.S.J., Moreci, R.S., Kyathanahalli, C., Hassan, S.S., Condon, J.C., et al., 2019. Steroidogenic factor 1 (Nr5a1) is required for sertoli cell survival post sex determination. Sci. Rep. 9 https://doi.org/10.1038/S41598-019-41051-1.

Ashburner, M., Ball, C.A., Blake, J.A., Botstein, D., Butler, H., Cherry, J.M., et al., 2000. Gene ontology: tool for the unification of biology. Nat. Genet. 25, 25–29. https://doi.org/10.1038/75556.

Aziz, M.H., Cui, K., Das, M., Brown, K.E., Ardell, C.L., Febbraio, M., et al., 2017. The upregulation of integrin α D β 2 (CD11d/CD18) on inflammatory macrophages promotes macrophage retention in vascular lesions and development of atherosclerosis. J. Immunol. 198, 4855–4867. https://doi.org/10.4049/JIMMUNOL.1602175.

Baba, T., Otake, H., Inoue, M., Sato, T., Ishihara, Y., Moon, J.Y., et al., 2018. Ad4BP/SF-1 regulates cholesterol synthesis to boost the production of steroids. Commun. Biol. 1 https://doi.org/10.1038/s42003-018-0020-z.

Balboa, D., Weltner, J., Eurola, S., Trokovic, R., Wartiovaara, K., Otonkoski, T., 2015. Conditionally stabilized dCas9 activator for controlling gene expression in human cell reprogramming and differentiation. Stem Cell Reports 5, 448–459. https://doi.org/10.1016/J.STEMCR.2015.08.001.

Bao, Y., Hudson, Q.J., Perera, E.M., Akan, L., Tobet, S.A., Smith, C.A., et al., 2009. Expression and evolutionary conservation of the tescalcin gene during development. Gene Expr. Patterns 9, 273–281. https://doi.org/10.1016/J.GEP.2009.03.004.

Bashamboo, A., Ferraz-De-Souza, B., Lourenço, D., Lin, L., Sebire, N.J., Montjean, D., et al., 2010. Human male infertility associated with mutations in NR5A1 encoding steroidogenic factor 1. Am. J. Hum. Genet. 87, 505–512. https://doi.org/10.1016/J.AJHG.2010.09.009.

Baxter, R.M., Arboleda, V.A., Lee, H., Barseghyan, H., Adam, M.P., Fechner, P.Y., et al., 2015. Exome sequencing for the diagnosis of 46, XY disorders of sex development. J. Clin. Endocrinol. Metab. 100, E333–E344. https://doi.org/10.1210/JC.2014-2605.

Benoit, G., Warma, A., Lussier, J.G., Ndiaye, K., 2019. Gonadotropin regulation of ankyrin-repeat and SOCS-box protein 9 (ASB9) in ovarian follicles and identification of binding partners. PLoS One 14. https://doi.org/10.1371/JOURNAL.PONE.0212571.

Bland, M.L., Fowkes, R.C., Ingraham, H.A., 2004. Differential requirement for steroidogenic factor-1 gene dosage in adrenal development versus endocrine function. Mol. Endocrinol. 18, 941–952. https://doi.org/10.1210/ME.2003-0333.

Bland, M.L., Jamieson, C., Akana, S., Dallman, M., Ingraham, H.A., 2000. Gene dosage effects of steroidogenic factor 1 (SF-1) in adrenal development and the stress. Endocr. Res. 26, 515–516. https://doi.org/10.3109/07435800009048563.

Buganim, Y., Itskovich, E., Hu, Y.C., Cheng, A.W., Ganz, K., Sarkar, S., et al., 2012. Direct reprogramming of fibroblasts into embryonic sertoli-like cells by defined factors. Cell Stem Cell 11, 373–386. https://doi.org/10.1016/J.STEM.2012.07.019.

Camats, N., Pandey, A.V., Fernández-Cancio, M., Andaluz, P., Janner, M., Torán, N., et al., 2012. Ten novel mutations in the NR5A1 gene cause disordered sex development in 46,XY and ovarian insufficiency in 46,XX individuals. J. Clin. Endocrinol. Metab. 97 https://doi.org/10.1210/JC.2011-3169.

Casarini, L., Crépieux, P., 2019. Molecular mechanisms of action of FSH. Front. Endocrinol. (Lausanne) 10. https://doi.org/10.3389/FENDO.2019.00305.

Cermak, T., Doyle, E.L., Christian, M., Wang, L., Zhang, Y., Schmidt, C., et al., 2011. Efficient design and assembly of custom TALEN and other TAL effector-based constructs for DNA targeting. Nucleic Acids Res 39. https://doi.org/10.1093/NAR/GKR218.

Chaboissier, M.C., Kobayashi, A., Vidal, V.I.P., Lützkendorf, S., van de Kant, H.J.G., Wegner, M., et al., 2004. Functional analysis os Sox8 and Sox9 during sex determination in the mouse. Development 131, 1891–1901. https://doi.org/10.1242/dev.01087.

Chen, M., Zhang, L., Cui, X., Lin, X., Li, Y., Wang, Y., et al., 2017. Wt1 directs the lineage specification of sertoli and granulosa cells by repressing Sf1 expression. Dev 144, 44–53. https://doi.org/10.1242/DEV.144105.

Chen, S., Shi, H., Liu, X., Segaloff, D.L., 1999. Multiple elements and protein factors coordinate the basal and cyclic adenosine 3',5'-monophosphate-induced transcription of the lutropin receptor gene in rat granulosa cells. Endocrinology 140, 2100–2109. https://doi.org/10.1210/ENDO.140.5.6722.

Cui, K., Ardell, C.L., Podolnikova, N.P., Yakubenko, V.P., 2018. Distinct migratory properties of M1, M2, and resident macrophages are regulated by αdβ2and αmβ2integrin-mediated adhesion. Front. Immunol. 9 https://doi.org/10.3389/FIMMU.2018.02650.

Curnow, K.M., Tusie-Lunaf, M.T., Pascoe, L., Natarajan, R., Gu, J.L., Nadler, J.L., et al., 1991. The product of the CYP11B2 gene is required for aldosterone biosynthesis in the human adrenal cortex. Mol. Endocrinol. 5, 1513–1522. https://doi.org/10.1210/MEND-5-10-1513.

Davis, A.P., Murphy, C.G., Saraceni-Richards, C.A., Rosenstein, M.C., Wiegers, T.C., Mattingly, C.J., 2009. Comparative Toxicogenomics Database: a knowledgebase and discovery tool for chemical-gene-disease networks. Nucleic Acids Res 37. https://doi.org/10.1093/NAR/GKN580.

De Robertis, M., Mazza, T., Fusilli, C., Loiacono, L., Poeta, M.L., Sanchez, M., et al., 2018. EphB2 stem-related and EphA2 progression-related miRNA-based networks in progressive stages of CRC evolution: clinical significance and potential miRNA drivers. Mol. Cancer 17. https://doi.org/10.1186/S12943-018-0912-Z.

DeFalco, T., Capel, B., 2009. Gonad morphogenesis in vertebrates: divergent means to a convergent end. Annu. Rev. Cell Dev. Biol. 25, 457–482. https://doi.org/10.1146/ANNUREV.CELLBIO.042308.13350.

del Valle, I., Buonocore, F., Duncan, A.J., Lin, L., Barenco, M., Parnaik, R., et al., 2017. A genomic atlas of human adrenal and gonad development. Wellcome open Res 2. https://doi.org/10.12688/WELLCOMEOPENRES.11253.2.

Doghman, M., Karpova, T., Rodrigues, G.A., Arhatte, M., De Moura, J., Cavalli, L.R., et al., 2007. Increased steroidogenic factor-1 dosage triggers adrenocortical cell proliferation and cancer. Mol. Endocrinol. 21, 2968–2987. https://doi.org/10.1210/me.2007-0120.

Domenice, S., Zamboni Machado, A., Moraes Ferreira, F., Ferraz-de-Souza, B., Marcondes Lerario, A., Lin, L., et al., 2016. Wide spectrum of NR5A1-related phenotypes in 46, XY and 46,XX individuals. Birth Defects Res. C. Embryo Today 108, 309–320. https://doi.org/10.1002/BDRC.21145.

Fabbri-Scallet, H., de Sousa, L.M., Maciel-Guerra, A.T., Guerra-Júnior, G., de Mello, M.P., 2020. Mutation update for the NR5A1 gene involved in DSD and infertility. Hum. Mutat. 41, 58–68. https://doi.org/10.1002/HUMU.23916.

Fukami, M., Wada, Y., Miyabayashi, K., Nishino, I., Hasegawa, T., Nordenskjöld, A., et al., 2006. CXorf6 is a causative gene for hypospadias. Nat. Genet. 38, 1369–1371. https://doi.org/10.1038/NG1900.

Fukami, M., Wada, Y., Okada, M., Kato, F., Katsumata, N., Baba, T., et al., 2008. Mastermind-like domain-containing 1 (MAMLD1 or CXorf6) transactivates the Hes3 promoter, augments testosterone production, and contains the SF1 target sequence. J. Biol. Chem. 283, 5525–5532. https://doi.org/10.1074/jbc.M703289200.

Georges, A., L'Hôte, D., Todeschini, A.L., Auguste, A., Legois, B., Zider, A., et al., 2014. The transcription factor FOXL2 mobilizes estrogen signaling to maintain the identity of ovarian granulosa cells. Elife 3, 1–19. https://doi.org/10.7554/ELIFE.04207.

Giuili, G., Shen, W.H., Ingraham, H.A., 1997. The nuclear receptor SF-1 mediates sexually dimorphic expression of Mullerian inhibiting substance, in vivo. Development 124, 1799–1807. https://doi.org/10.1242/dev.124.9.1799.

Givens, C.R., Zhang, P., Bair, S.R., Mellon, S.H., 1994. Transcriptional regulation of rat cytochrome P450c17 expression in mouse Leydig MA-10 and adrenal Y-1 cells: identification of a single protein that mediates both basal and cAMP-induced activities. DNA Cell Biol 13, 1087–1098. https://doi.org/10.1089/DNA.1994.13.1087.

Goertsches, R., Comabella, M., Navarro, A., Perkal, H., Montalban, X., 2005. Genetic association between polymorphisms in the ADAMTS14 gene and multiple sclerosis. J. Neuroimmunol. 164, 140–147. https://doi.org/10.1016/j.jneuroim.2005.04.005.

Grayson, M.H., Van Der Vieren, M., Sterbinsky, S.A., Gallatin, W.M., Hoffman, P.A., Staunton, D.E., et al., 1998. αdβ2 integrin is expressed on human eosinophils and functions as an alternative ligand for vascular cell adhesion molecule 1 (VCAM-1). J. Exp. Med. 188, 2187–2191. https://doi.org/10.1084/JEM.188.11.2187.

Gregory, C.W., DePhilip, R.M., 1998. Detection of Steroidogenic Acute Regulatory protein (StAR) in mitochondria of cultured rat Sertoli cells incubated with follicle-stimulating hormone. Biol. Reprod. 58, 470–474. https://doi.org/10.1095/BIOLREPROD58.2.470.

Guo, J., Sosa, E., Chitiashvili, T., Nie, X., Rojas, E.J., Oliver, E., et al., 2021. Single-cell analysis of the developing human testis reveals somatic niche cell specification and fetal germline stem cell establishment. Cell Stem Cell 28, 764–778. https://doi.org/10.1016/J.STEM.2020.12.004.

Hanley, N.A., Ball, S.G., Clement-Jones, M., Hagan, D.M., Strachan, T., Lindsay, S., et al., 1999. Expression of steroidogenic factor 1 and Wilms' tumour 1 during early human gonadal development and sex determination. Mech. Dev. 87, 175–180. https://doi.org/10.1016/S0925-4773(99)00123-9.

Hatano, O., Takakusu, A., Nomura, M., Morohashi, K.I., 1996. Identical origin of adrenal cortex and gonad revealed by expression profiles of Ad4BP/SF-1. Genes to Cells 1, 663–671. https://doi.org/10.1046/J.1365-2443.1996.00254.X.

Heckert, L.L., 2001. Activation of the rat follicle-stimulating hormone receptor promoter by steroidogenic factor 1 is blocked by protein kinase A and requires upstream stimulatory factor binding to a proximal E box element. Mol. Endocrinol. 15, 704–715. https://doi.org/10.1210/MEND.15.5.0632.

Heese, K., Nagai, Y., Sawada, T., 2003. Comparative gene identification-94 - a pivotal regulator of apoptosis. Neuroscience 116, 321–324. https://doi.org/10.1016/S0306-4522(02)00653-X.

Heese, K., Nakayama, T., Hata, R., Masumura, M., Akatsu, H., Li, F., et al., 2002. Characterizing CGI-94 (comparative gene identification-94) which is down-regulated in the hippocampus of early stage Alzheimer's disease brain. Eur. J. Neurosci. 15, 79–86. https://doi.org/10.1046/j.0953-816x.2001.01836.x.

Hu, M.C., Hsu, N.C., Pai, C.I., Leo Wang, C.K., Chung, B.C., 2001. Functions of the upstream and proximal steroidogenic factor 1 (SF-1)-binding sites in the CYP11A1 promoter in basal transcription and hormonal response. Mol. Endocrinol. 15, 812–818. https://doi.org/10.1210/MEND.15.5.0636.

Hu, Y.C., Okumura, L.M., Page, D.C., 2013. Gata4 is required for formation of the genital ridge in mice. PLoS Genet 9. https://doi.org/10.1371/JOURNAL.PGEN.1003629.

Huang, D.W., Sherman, B.T., Lempicki, R.A., 2009a. Bioinformatics enrichment tools: paths toward the comprehensive functional analysis of large gene lists. Nucleic Acids Res 37, 1–13. https://doi.org/10.1093/NAR/GKN923.

Huang, D.W., Sherman, B.T., Lempicki, R.A., 2009b. Systematic and integrative analysis of large gene lists using DAVID bioinformatics resources. Nat. Protoc. 4, 44–57. https://doi.org/10.1038/nprot.2008.211.

Huang, J., Zheng, D.L., Qin, F.S., Cheng, N., Chen, H., Wan, B.B., et al., 2010. Genetic and epigenetic silencing of SCARA5 may contribute to human hepatocellular carcinoma by activating FAK signaling. J. Clin. Invest. 120, 223–241. https://doi.org/10.1172/JCI38012.

Ikeda, Y., Shen, W.H., Ingraham, H.A., Parker, K.L., 1994. Developmental expression of mouse steroidogenic factor-1, an essential regulator of the steroid hydroxylases. Mol. Endocrinol. 8, 654–662. https://doi.org/10.1210/MEND.8.5.8058073.

Ikeda, Y., Tagami, A., Maekawa, M., Nagai, A., 2021. The conditional deletion of steroidogenic factor 1 (Nr5a1) in Sox9-Cre mice compromises testis differentiation. Sci. Rep. 11 https://doi.org/10.1038/S41598-021-84095-Y.

Ikeda, Y., Takeda, Y., Shikayama, T., Mukai, T., Hisano, S., Morohashi, K.I., 2001. Comparative localization of Dax-1 and Ad4BP/SF-1 during development of the hypothalamic-pituitary-gonadal axis suggests their closely related and distinct functions. Dev. Dyn. 220, 363–376. https://doi.org/10.1002/DVDY.1116.

Imtiaz, A., Belyantseva, I.A., Beirl, A.J., Fenollar-Ferrer, C., Bashir, R., Bukhari, I., et al., 2018. CDC14A phosphatase is essential for hearing and male fertility in mouse and human. Hum. Mol. Genet. 27, 780–798. https://doi.org/10.1093/HMG/DDX440.

Jadhav, U., Jameson, J.L., 2011. Steroidogenic factor-1 (SF-1)-driven differentiation of murine embryonic stem (ES) cells into a gonadal lineage. Endocrinology 152, 2870–2882. https://doi.org/10.1210/EN.2011-0219.

Ji, S.Y., Hao, J.X., Li, L., Zhang, J., Zheng, Q.S., Li, X.X., et al., 2013. Expression of inhibin-alpha is regulated synergistically by wilms' tumor gene 1 (Wt1) and steroidogenic factor-1 (Sf1) in sertoli cells. PLoS One 8. https://doi.org/10.1371/JOURNAL.PONE.0053140.

Jiang, Y., Oliver, P., Davies, K.E., Platt, N., 2006. Identification and characterization of murine SCARA5, a novel class A scavenger receptor that is expressed by populations of epithelial cells. J. Biol. Chem. 281, 11834–11845. https://doi.org/10.1074/jbc.M507599200.

Jin, H., Won, M., Park, S.E., Lee, S., Park, M., Bae, J., 2016. FOXL2 is an essential activator of SF-1-Induced transcriptional regulation of anti-müllerian hormone in human granulosa cells. PLoS One 11. https://doi.org/10.1371/JOURNAL.PONE.0159112.

Johnston, H., Baker, P.J., Abel, M., Charlton, H.M., Jackson, G., Fleming, L., et al., 2004. Regulation of sertoli cell number and activity by follicle-stimulating hormone and androgen during postnatal development in the mouse. Endocrinology 145, 318–329. https://doi.org/10.1210/EN.2003-1055.

Kashimada, K., Svingen, T., Feng, C., Pelosi, E., Bagheri-Fam, S., Harley, V.R., et al., 2011. Antagonistic regulation of Cyp26b1 by transcription factors SOX9/SF1 and FOXL2 during gonadal development in mice. FASEB J 25, 3561–3569. https://doi.org/10.1096/FJ.11-184333.

Kreidberg, J.A., Sariola, H., Loring, J.M., Maeda, M., Pelletier, J., Housman, D., et al., 1993. WT-1 is required for early kidney development. Cell 74, 679–691. https://doi.org/10.1016/0092-8674(93)90515-R.

Lee, H., Lee, Y.J., Choi, H., Seok, J.W., Yoon, B.K., Kim, D., et al., 2017. SCARA5 plays a critical role in the commitment of mesenchymal stem cells to adipogenesis. Sci. Rep. 7 https://doi.org/10.1038/S41598-017-12512-2.

Lee, S.Y., Lee, H.S., Gil, M., Kim, C.J., Lee, Y.H., Kim, K.R., et al., 2014. Differential expression patterns of a disintegrin and metalloproteinase with thrombospondin motifs (adamts) -1, -4, -5, and -14 in human placenta and gestational trophoblastic diseases. Arch. Pathol. Lab. Med. 138, 643–650. https://doi.org/10.5858/ARPA.2012-0227-OA.

Leng, N., Li, Y., McIntosh, B.E., Nguyen, B.K., Duffin, B., Tian, S., et al., 2015. EBSeq-HMM: a Bayesian approach for identifying gene-expression changes in ordered RNA-seq experiments. Bioinformatics 31, 2614–2622. https://doi.org/10.1093/bioinformatics/btv193.

Li, J.Y., Paragas, N., Ned, R.M., Qiu, A., Viltard, M., Leete, T., et al., 2009. Scara5 is a ferritin receptor mediating non-transferrin iron delivery. Dev. Cell 16, 35–46. https://doi.org/10.1016/J.DEVCEL.2008.12.002.

Li, X., Liu, Y., Kay, C.M., Müller-Esterl, W., Fliegel, L., 2003. The Na+/H+ exchanger cytoplasmic tail: structure, function, and interactions with tescalcin. Biochemistry 42, 7448–7456. https://doi.org/10.1021/BI027143D.

Liang, J., Wang, N., He, J., Du, J., Guo, Y., Li, L., et al., 2019. Induction of Sertoli-like cells from human fibroblasts by NR5A1 and GATA4. Elife 8. https://doi.org/10.7554/ELIFE.48767.

Lin, Y.M., Lin, C.W., Lu, J.W., Yeh, K.T., Lin, S.H., Yang, S.F., 2020. Decreased cytoplasmic expression of ADAMTS14 is correlated with reduced survival rates in oral squamous cell carcinoma patients. Diagnostics 10. https://doi.org/10.3390/DIAGNOSTICS10020122.

Liu, J., Hu, G., Chen, D., Gong, A.Y., Soori, G.S., Dobleman, T.J., et al., 2013. Suppression of SCARA5 by Snail1 is essential for EMT-associated cell migration of A549 cells. Oncogenesis 2. https://doi.org/10.1038/ONCSIS.2013.37.

Liu, W., He, X., Yang, S., Zouari, R., Wang, J., Wu, H., et al., 2019. Bi-Allelic mutations in TTC21A induce asthenoteratospermia in humans and mice. Am. J. Hum. Genet. 104, 738–748. https://doi.org/10.1016/j.ajhg.2019.02.020.

Livak, K.J., Schmittgen, T.D., 2001. Analysis of relative gene expression data using real-time quantitative PCR and the 2-ΔΔCT method. Methods 25, 402–408. https://doi.org/10.1006/METH.2001.1262.

Lottrup, G., Belling, K., Leffers, H., Nielsen, J.E., Dalgaard, M.D., Juul, A., et al., 2017. Comparison of global gene expression profiles of microdissected human foetal Leydig cells with their normal and hyperplastic adult equivalents. Mol. Hum. Reprod. 23, 339–354. https://doi.org/10.1093/MOLEHR/GAX012.

Lourenço, D., Brauner, R., Lin, L., De Perdigo, A., Weryha, G., Muresan, M., et al., 2009. Mutations in NR5A1 associated with ovarian insufficiency. N. Engl. J. Med. 360, 1200–1210. https://doi.org/10.1056/NEJMOA0806228.

Love, M.I., Huber, W., Anders, S., 2014. Moderated estimation of fold change and dispersion for RNA-seq data with DESeq2. Genome Biol 15. https://doi.org/10.1186/s13059-014-0550-8.

Luo, X., Ikeda, Y., Parker, K.L., 1994. A cell-specific nuclear receptor is essential for adrenal and gonadal development and sexual differentiation. Cell 77, 481–490. https://doi.org/10.1016/0092-8674(94)90211-9.

Lurquin, C., De Smet, C., Brasseur, F., Muscatelli, F., Martelange, V., De Plaen, E., et al., 1997. Two members of the human MAGEB gene family located in Xp21.3 are expressed in tumors of various histological origins. Genomics 46, 397–408. https://doi.org/10.1006/geno.1997.5052.

Maciel, F.C., Maloberti, P., Neuman, I., Cano, F., Castilla, R., Castillo, F., et al., 2005. An arachidonic acid-preferring acyl-CoA synthetase is a hormone-dependent and obligatory protein in the signal transduction pathway of steroidogenic hormones. J. Mol. Endocrinol. 34, 655–666. https://doi.org/10.1677/jme.1.01691.

Maguire, S.M., Tribley, W.A., Griswold, M.D., 1997. Follicle-stimulating hormone (FSH) regulates the expression of FSH receptor messenger ribonucleic acid in cultured Sertoli cells and in hypophysectomized rat testis. Biol. Reprod. 56, 1106–1111. https://doi.org/10.1095/BIOLREPROD56.5.1106.

Mailänder, J., Müller-Esterl, W., Dedio, J., 2001. Human homolog of mouse tescalcin associates with Na+/H+ exchanger type-1. FEBS Lett 507, 331–335. https://doi.org/10.1016/S0014-5793(01)02986-6.

Mallet, D., Bretones, P., Michel-Calemard, L., Dijoud, F., David, M., Morel, Y., 2004. Gonadal dysgenesis without adrenal insufficiency in a 46, XY patient heterozygous for the nonsense C16X mutation: a case of SF1 haploinsufficiency. J. Clin. Endocrinol. Metab. 89, 4829–4832. https://doi.org/10.1210/jc.2004-0670.

Matys, V., Fricke, E., Geffers, R., Gößling, E., Haubrock, M., Hehl, R., et al., 2003. TRANSFAC®: transcriptional regulation, from patterns to profiles. Nucleic Acids Res 31, 374–378. https://doi.org/10.1093/NAR/GKG108.

McDonald, C.A., Millena, A.C., Reddy, S., Finlay, S., Vizcarra, J., Khan, S.A., et al., 2006. Follicle-stimulating hormone-induced aromatase in immature rat sertoli cells requires an active phosphatidylinositol 3-kinase pathway and is inhibited via the mitogen-activated protein kinase signaling pathway. Mol. Endocrinol. 20, 608–618. https://doi.org/10.1210/me.2005-0245.

Melau, C., Nielsen, J.E., Frederiksen, H., Kilcoyne, K., Perlman, S., Lundvall, L., et al., 2019. Characterization of human adrenal steroidogenesis during fetal development. J. Clin. Endocrinol. Metab. 104, 1802–1812. https://doi.org/10.1210/JC.2018-01759.

Michael, M.D., Kilgore, M.W., Morohashi, K.I., Simpson, E.R., 1995. Ad4BP/SF-1 regulates cyclic AMP-induced transcription from the proximal promoter (PII) of the human aromatase P450 (CYP19) gene in the ovary. J. Biol. Chem. 270, 13561–13566. https://doi.org/10.1074/JBC.270.22.13561.

Migrenne, S., Moreau, E., Pakarinen, P., Dierich, A., Merlet, J., Habert, R., et al., 2012. Mouse testis development and function are differently regulated by follicle-stimulating hormone receptors signaling during fetal and prepubertal Life. PLoS One 7. https://doi.org/10.1371/JOURNAL.PONE.0053257.

Miller, W.L., Auchus, R.J., 2011. The molecular biology, biochemistry, and physiology of human steroidogenesis and its disorders. Endocr. Rev. 32, 81–151. https://doi.org/10.1210/ER.2010-0013.

Miyado, M., Yoshida, K., Miyado, K., Katsumi, M., Saito, K., Nakamura, S., et al., 2017. Knockout of murine Mamld1 impairs testicular growth and daily sperm production but permits normal postnatal androgen production and fertility. Int. J. Mol. Sci. 18 https://doi.org/10.3390/IJMS18061300.

Morohashi, K., Omura, T., 1996. Ad4BP/SF-1, a transcription factor essential for the transcription of steroidogenic cytochrome P450 genes and for the establishment of the reproductive function. FASEB J 10, 1569–1577. https://doi.org/10.1096/FASEBJ.10.14.9002548.

Mullican, S.E., DiSpirito, J.R., Lazar, M.A., 2013. The orphan nuclear receptors at their 25-year reunion. J. Mol. Endocrinol. 51 https://doi.org/10.1530/JME-13-0212.

Muscatelli, F., Walker, A.P., De Plaen, E., Stafford, A.N., Monaco, A.P., 1995. Isolation and characterization of a MAGE gene family in the Xp21.3 region. Proc. Natl. Acad. Sci. U. S. A. 92, 4987–4991. https://doi.org/10.1073/PNAS.92.11.4987.

O'Shaughnessy, P.J., Baker, P.J., Heikkilä, M., Vainio, S., Mcmahon, A.P., 2000. Localization of 17β-hydroxysteroid dehydrogenase/17-ketosteroid reductase isoform expression in the developing mouse testis - androstenedione is the major androgen secreted by fetal/neonatal Leydig cells. Endocrinology 141, 2631–2637. https://doi.org/10.1210/ENDO.141.7.7545.

O'Shaughnessy, P.J., Fowler, P.A., 2011. Endocrinology of the mammalian fetal testis. Reproduction 141, 37–46. https://doi.org/10.1530/REP-10-0365.

Ogishima, T., Mitani, F., Ishimura, Y., 1989. Isolation of aldosterone synthase cytochrome P-450 from zona glomerulosa mitochondria of rat adrenal cortex. J. Biol. Chem. 264, 10935–10938. https://doi.org/10.1016/s0021-9258(18)60408-9.

Ohlsson, C., Langenskiöld, M., Smidfelt, K., Poutanen, M., Ryberg, H., Norlén, A.-K., et al., 2021. Low progesterone and low estradiol levels associate with abdominal aortic aneurysms in men. J. Clin. Endocrinol. Metab. XX, 1–13. https://doi.org/10.1210/CLINEM/DGAB867.

Orth, J.M., 1984. The role of follicle-stimulating hormone in controlling Sertoli cell proliferation in testes of fetal rats. Endocrinology 115, 1248–1255. https://doi.org/10.1210/ENDO-115-4-1248.

Ouni, E., Bouzin, C., Dolmans, M.M., Marbaix, E., Pyr Dit Ruys, S., Vertommen, D., et al., 2020. Spatiotemporal changes in mechanical matrisome components of the human ovary from prepuberty to menopause. Hum. Reprod. 35, 1391–1410. https://doi.org/10.1093/HUMREP/DEAA100.

Park, M., Shin, E., Won, M., Kim, J.H., Go, H., Kim, H.L., et al., 2010. FOXL2 interacts with steroidogenic factor-1 (SF-1) and represses SF-1-induced CYP17 transcription in granulosa cells. Mol. Endocrinol. 24, 1024–1036. https://doi.org/10.1210/ME.2009-0375.

Perälä, N.M., Immonen, T., Sariola, H., 2005. The expression of plexins during mouse embryogenesis. Gene Expr. Patterns 5, 355–362. https://doi.org/10.1016/j.modgep.2004.10.001.

Perera, E.M., Martin, H., Seeherunvong, T., Kos, L., Hughes, I.A., Hawkins, J.R., et al., 2001. Tescalcin, a novel gene encoding a putative EF-hand Ca2+-binding protein, Col9a3, and Renin are expressed in the mouse testis during the early stages of gonadal differentiation. Endocrinology 142, 455–463. https://doi.org/10.1210/endo.142.1.7882.

Porter, S., Scott, S.D., Sassoon, E.M., Williams, M.R., Jones, J.L., Girling, A.C., et al., 2004. Dysregulated expression of adamalysin-thrombospondin genes in human breast carcinoma. Clin. Cancer Res. 10, 2429–2440. https://doi.org/10.1158/1078-0432.CCR-0398-3.

Rajpert-De Meyts, E., Jørgensen, N., Græm, N., Müller, J., Cate, R.L., Skakkebæk, N.E., 1999. Expression of anti-Mullerian hormone during normal and pathological gonadal development: association with differentiation of Sertoli and granulosa cells. J. Clin. Endocrinol. Metab. 84, 3836–3844. https://doi.org/10.1210/jc.84.10.3836.

Ramaswamy, S., Weinbauer, G.F., 2015. Endocrine control of spermatogenesis: role of FSH and LH/testosterone. Spermatogenesis 4, e996025. https://doi.org/10.1080/21565562.2014.996025.

Rannikko, A.S., Zhang, F.P., Huhtaniemi, I.T., 1995. Ontogeny of follicle-stimulating hormone receptor gene expression in the rat testis and ovary. Mol. Cell. Endocrinol. 107, 199–208. https://doi.org/10.1016/0303-7207(94)03444-X.

Rhéaume, E., Lachance, Y., Zhao, H.F., Breton, N., Dumont, M., de Launoit, Y., et al., 1991. Structure and expression of a new complementary DNA encoding the almost exclusive 3β-hydroxysteroid dehydrogenase/Δ5-Δ4-Isomerase in Human adrenals and gonads. Mol. Endocrinol. 5, 1147–1157. https://doi.org/10.1210/mend-5-8-1147.

Rodriguez-Lopez, J., Pombo-Suarez, M., Loughlin, J., Tsezou, A., Blanco, F.J., Meulenbelt, I., et al., 2009. Association of a nsSNP in ADAMTS14 to some osteoarthritis phenotypes. Osteoarthr. Cartil. 17, 321–327. https://doi.org/10.1016/j.joca.2008.07.012.

Rore, H., Owen, N., Piña-Aguilar, R.E., Docherty, K., Sekido, R., 2021. Testicular somatic cell-like cells derived from embryonic stem cells induce differentiation of epiblasts into germ cells. Commun. Biol. 4 https://doi.org/10.1038/s42003-021-02322-8.

Rotgers, E., Jørgensen, A., Yao, H.H.C., 2018. At the crossroads of fate-Somatic cell lineage specification in the fetal gonad. Endocr. Rev. 39, 739–759. https://doi.org/10.1210/er.2018-00010.

Rouillard, A.D., Gundersen, G.W., Fernandez, N.F., Wang, Z., Monteiro, C.D., McDermott, M.G., et al., 2016. The Harmonizome: a Collection of Processed Datasets Gathered to Serve and Mine Knowledge about Genes and Proteins. Database, Oxford). https://doi.org/10.1093/database/baw100, 2016.

Sadate-Ngatchou, P.I., Pouchnik, D.J., Griswold, M.D., 2004. Follicle-stimulating hormone induced changes in gene expression of murine testis. Mol. Endocrinol. 18, 2805–2816. https://doi.org/10.1210/me.2003-0203.

Sadovsky, Y., Crawford, P.A., Woodson, K.G., Polish, J.A., Clements, M.A., Tourtellotte, L.M., et al., 1995. Mice deficient in the orphan receptor steroidogenic factor 1 lack adrenal glands and gonads but express P450 side-chain-cleavage enzyme in the placenta and have normal embryonic serum levels of corticosteroids. Proc. Natl. Acad. Sci. U. S. A. 92, 10939–10943. https://doi.org/10.1073/pnas.92.24.10939.

Sarkar, M., Schilffarth, S., Schams, D., Meyer, H.H.D., Berisha, B., 2011. The expression of thrombopoietin and its receptor during different physiological stages in the bovine ovary. Reprod. Domest. Anim. 46, 757–762. https://doi.org/10.1111/j.1439-0531.2010.01736.x.

Sarraj, M.A., McClive, P.J., Wilmore, H.P., Loveland, K.L., Sinclair, A.H., 2005. Novel scavenger receptor gene is differentially expressed in the embryonic and adult mouse testis. Dev. Dyn. 234, 1026–1033. https://doi.org/10.1002/dvdy.20594.

Sasaki, K., Oguchi, A., Cheng, K., Murakawa, Y., Okamoto, I., Ohta, H., et al., 2021. The embryonic ontogeny of the gonadal somatic cells in mice and monkeys. Cell Rep 35. https://doi.org/10.1016/j.celrep.2021.109075.

Satoh, M., 1991. Histogenesis and organogenesis of the gonad in human embryos. J. Anat. 177, 85–107. https://doi.org/10.1007/BF02349668.

Savchuk, I., Morvan, M.L., Antignac, J.P., Kurek, M., Le Bizec, B., Söder, O., et al., 2019. Ontogenesis of human fetal testicular steroidogenesis at early gestational age. Steroids 141, 96–103. https://doi.org/10.1016/j.steroids.2018.12.001.

Schindler, K., Schultz, R.M., 2009. The CDC14A phosphatase regulates oocyte maturation in mouse. Cell Cycle 8, 1090–1098. https://doi.org/10.4161/cc.8.7.8144.

Schmahl, J., Eicher, E.M., Washburn, L.L., Capel, B., 2000. Sry induces cell proliferation in the mouse gonad. Development 127, 65–73. https://doi.org/10.1242/dev.127.1.65.

Sekido, R., Lovell-Badge, R., 2008. Sex determination involves synergistic action of SRY and SF1 on a specific Sox9 enhancer. Nature 453, 930–934. https://doi.org/10.1038/nature06944.

Sepponen, K., Lundin, K., Knuus, K., Väyrynen, P., Raivio, T., Tapanainen, J.S., et al., 2017. The role of sequential BMP signaling in directing human embryonic stem cells to bipotential gonadal cells. J. Clin. Endocrinol. Metab. 102, 4303–4314. https://doi.org/10.1210/jc.2017-01469.

Shao, X., Liao, J., Lu, X., Xue, R., Ai, N., Fan, X., 2020. scCATCH: automatic annotation on cell types of clusters from single-cell RNA sequencing data. iScience 23. https://doi.org/10.1016/j.isci.2020.100882.

She, Z.Y., Yang, W.X., 2017. Sry and SoxE genes: how they participate in mammalian sex determination and gonadal development? Semin. Cell Dev. Biol. 63, 13–22. https://doi.org/10.1016/j.semcdb.2016.07.032.

Shen, W.H., Moore, C.C.D., Ikeda, Y., Parker, K.L., Ingraham, H.A., 1994. Nuclear receptor steroidogenic factor 1 regulates the müllerian inhibiting substance gene: a link to the sex determination cascade. Cell 77, 651–661. https://doi.org/10.1016/0092-8674(94)90050-7.

Shima, Y., Miyabayashi, K., Haraguchi, S., Arakawa, T., Otake, H., Baba, T., et al., 2013. Contribution of Leydig and Sertoli cells to testosterone production in mouse fetal testes. Mol. Endocrinol. 27, 63–73. https://doi.org/10.1210/me.2012-1256.

Siegers, G.M., Barreira, C.R., Postovit, L.-M., Dekaban, G.A., 2017. CD11d β2 integrin expression on human NK, B, and γδ T cells. J. Leukoc. Biol. 101, 1029–1035. https://doi.org/10.1189/jlb.3ab0716-326rr.

Souquet, B., Tourpin, S., Messiaen, S., Moison, D., Habert, R., Livera, G., 2012. Nodal signaling regulates the entry into meiosis in fetal germ cells. Endocrinology 153, 2466–2473. https://doi.org/10.1210/en.2011-2056.

Spiller, C.M., Feng, C.W., Jackson, A., Gillis, A.J.M., Rolland, A.D., Looijenga, L.H.J., et al., 2012. Endogenous Nodal signaling regulates germ cell potency during mammalian testis development. Dev 139, 4123–4132. https://doi.org/10.1242/dev.083006.

Stévant, I., Kühne, F., Greenfield, A., Chaboissier, M.C., Dermitzakis, E.T., Nef, S., 2019. Dissecting cell lineage specification and sex fate determination in gonadal somatic cells using single-cell transcriptomics. Cell Rep 26, 3272–3283. https://doi.org/10.1016/j.celrep.2019.02.069 e3.

Stévant, I., Neirijnck, Y., Borel, C., Escoffier, J., Smith, L.B., Antonarakis, S.E., et al., 2018. Deciphering cell lineage specification during male sex determination with single-cell RNA sequencing. Cell Rep 22, 1589–1599. https://doi.org/10.1016/j.celrep.2018.01.043.

Strizzi, L., Bianco, C., Normanno, N., Salomon, D., 2005. Cripto-1: a multifunctional modulator during embryogenesis and oncogenesis. Oncogene 24, 5731–5741. https://doi.org/10.1038/sj.onc.1208918.

Takasawa, K., Kashimada, K., Pelosi, E., Takagi, M., Morio, T., Asahara, H., et al., 2014. FOXL2 transcriptionally represses Sf1 expression by antagonizing WT1 during ovarian development in mice. FASEB J 28, 2020–2028. https://doi.org/10.1096/fj.13-246108.

Tang, F., Richardson, N., Albina, A., Chaboissier, M.C., Perea-Gomez, A., 2020. Mouse gonad development in the absence of the pro-ovary factor WNT4 and the pro-testis factor SOX9. Cells 9. https://doi.org/10.3390/cells9051103.

Tran, D., Josso, N., Meusy-dessolle, N., 1977. Anti-Müllerian hormone is a functional marker of foetal Sertoli cells. Nature 269, 411–412. https://doi.org/10.1038/269411a0.

Triebner, K., Bifulco, E., Real, F., Hustad, S., 2014. A sensitive method for estrogen profiling in human serum by liquid chromatography-tandem mass spectrometry. Endocr. Abstr. 35 https://doi.org/10.1530/ENDOABS.35.P647.

Turcu, A.F., Auchus, R.J., 2015. Adrenal steroidogenesis and congenital adrenal hyperplasia. Endocrinol. Metab. Clin. North Am. 44, 275–296. https://doi.org/10.1016/j.ecl.2015.02.002.

Vainio, S., Heikkilä, M., Kispert, A., Chin, N., McMahon, A.P., 1999. Female development in mammals is regulated by Wnt-4 signalling. Nature 397, 405–409. https://doi.org/10.1038/17068.

Van der Vieren, M., Crowe, D.T., Hoekstra, D., Vazeux, R., Hoffman, P.A., Grayson, M.H., et al., 1999. The leukocyte integrin alpha D beta 2 binds VCAM-1: evidence for a binding interface between I domain and VCAM-1. J. Immunol 163, 1984. –90. Available at: http://www.ncbi.nlm.nih.gov/pubmed/10438935. (Accessed 25 November 2021).

Van der Vieren, M., Le Trong, H., Wood, C.L., Moore, P.F., John, T.S., Staunton, D.E., et al., 1995. A novel leukointegrin, αdβ2, binds preferentially to ICAM-3. Immunity 3, 683–690. https://doi.org/10.1016/1074-7613(95)90058-6.

Voutilainen, R., Miller, W.L., 1986. Developmental expression of genes for the stereoidogenic enzymes P450scc (20,22-desmolase), P450cl7 (17αhydroxylase/17,20-lyase), and P450c21 (21-hydroxylase) in the human fetusxsxs. J. Clin. Endocrinol. Metab. 63, 1145–1150. https://doi.org/10.1210/jcem-63-5-1145.

Watanabe, K., Clarke, T.R., Lane, A.H., Wang, X., Donahoe, P.K., 2000. Endogenous expression of müllerian inhibiting substance in early postnatal rat sertoli cells requires multiple steroidogenic factor-1 and GATA-4-binding sites. Proc. Natl. Acad. Sci. U. S. A. 97, 1624–1629. https://doi.org/10.1073/pnas.97.4.1624.

Welsh, M.J., Wiebe, J.P., 1976. Sertoli cells from immature rats: in vitro stimulation of steroid metabolism by FSH. Biochem. Biophys. Res. Commun. 69, 936–941. https://doi.org/10.1016/0006-291X(76)90463-0.

Weltner, J., Balboa, D., Katayama, S., Bespalov, M., Krjutškov, K., Jouhilahti, E.M., et al., 2018. Human pluripotent reprogramming with CRISPR activators. Nat. Commun. 9 https://doi.org/10.1038/s41467-018-05067-x.

Wen, X., Wang, N., Zhang, F., Dong, C., 2016. Overexpression of SCARA5 inhibits tumor proliferation and invasion in osteosarcoma via suppression of the FAK signaling pathway. Mol. Med. Rep. 13, 2885–2891. https://doi.org/10.3892/mmr.2016.4857.

Wen, Z., Zhu, H., Zhang, A., Lin, J., Zhang, G., Liu, D., et al., 2020. Cdc14a has a role in spermatogenesis, sperm maturation and male fertility. Exp. Cell Res. 395 https://doi.org/10.1016/j.yexcr.2020.112178.

Wong, D.A., Davis, E.M., LeBeau, M., Springer, T.A., 1996. Cloning and chromosomal localization of a novel gene-encoding a human β2-integrin α subunit. Gene 171, 291–294. https://doi.org/10.1016/0378-1119(95)00869-1.

Yoshimoto, F.K., Auchus, R.J., 2015. The diverse chemistry of cytochrome P450 17A1 (P450c17, CYP17A1). J. Steroid Biochem. Mol. Biol. 151, 52–65. https://doi.org/10.1016/j.jsbmb.2014.11.026.

You, K., Su, F., Liu, L., Lv, X., Zhang, J., Zhang, Y., et al., 2017. SCARA5 plays a critical role in the progression and metastasis of breast cancer by inactivating the ERK1/2, STAT3, and AKT signaling pathways. Mol. Cell. Biochem. 435, 47–58. https://doi.org/10.1007/s11010-017-3055-4.

Zanetti, M., Braghetta, P., Sabatelli, P., Mura, I., Doliana, R., Colombatti, A., et al., 2004. EMILIN-1 deficiency induces elastogenesis and vascular cell defects. Mol. Cell. Biol. 24, 638–650. https://doi.org/10.1128/mcb.24.2.638-650.2004.

Zhang, P., Mellon, S.H., 1996. The orphan nuclear receptor steroidogenic factor-1 regulates the cyclic adenosine 3′,5′-monophosphate-mediated transcriptional activation of rat cytochrome P450c17 (17α-hydroxylase/c17-20 lyase). Mol. Endocrinol. 10, 147–158. https://doi.org/10.1210/mend.10.2.8825555.

Zhao, H.F., Labrie, C., Simard, J., De Launoit, Y., Trudel, C., Martel, C., et al., 1991. Characterization of rat 3β-hydroxysteroid dehydrogenase/Δ5-Δ4 isomerase cDNAs and differential tissue-specific expression of the corresponding mRNAs in steroidogenic and peripheral tissues. J. Biol. Chem. 266, 583–593. https://doi.org/10.1016/s0021-9258(18)52475-3.

Zubair, M., Oka, S., Parker, K.L., Morohashi, K.I., 2009. Transgenic expression of Ad4BP/SF-1 in fetal adrenal progenitor cells leads to ectopic adrenal formation. Mol. Endocrinol. 23, 1657–1667. https://doi.org/10.1210/me.2009-0055.